LRP 805/05 July 2005

Report on the Conceptual Design of External HTS Bus Bars

EFDA Reference: TW4-TMSF-HTSCOM
(Deliverable 2)

R. Wesche, R. Heller, W.H. Fietz, V.L. Tanna
and G. Zahn

ISSN 0458-5895

CENTRE DE RECHERCHES EN PHYSIQUE DES PLASMAS
ASSOCIATION EURATOM - CONFEDERATION SUISSE
CRPP - Technologie de la Fusion, CH - 5232 Villigen PSI

ÉCOLE POLYTECHNIQUE
FÉDÉRALE DE LAUSANNE

Report on the Conceptual Design of External HTS Bus Bars

EFDA Reference: TW4-TMSF-HTSCOM

Deliverable 2

R. Wesche[1], R. Heller[2], W.H. Fietz[2], V.L. Tanna[2], and G. Zahn[2]

[1]Centre de Recherches en Physique des Plasmas, Villigen, Switzerland

[2]Forschungszentrum Karlsruhe, Institut für Technische Physik, Karlsruhe, Germany

June 2005

Centre de Recherches en Physique des Plasmas

Internal Report

Report on the Conceptual Design of External HTS Bus Bars

EFDA Reference: TW4-TMSF-HTSCOM

Deliverable 2

R. Wesche[1], R. Heller[2], W.H. Fietz[2], V.L. Tanna[2], and G. Zahn[2]

[1]Centre de Recherches en Physique des Plasmas, Villigen, Switzerland

[2]Forschungszentrum Karlsruhe, Institut für Technische Physik, Karlsruhe, Germany

Table of Contents

Foreword

The task "Conceptual Design of External HTS Bus Bars" (EFDA Reference: TW4-TMSF-HTSCOM) is a joint work between the Centre de Recherches en Physique des Plasmas (CRPP), Villigen, Switzerland, and the Forschungszentrum Karlsruhe, Germany. The two main objectives of the task TW4-TMSF-HTSCOM are:

a) Comparison of the actual ITER design with and without HTS current leads.

b) Consequences of the use of HTS current leads and HTS bus bars for ITER including a conceptual design of the external HTS bus bars.

The work performed at the Forschungszentrum Karlsruhe focuses on the potential advantages of the use of HTS current leads instead of conventional ones for ITER, while CRPP considers the consequences of the use of HTS bus bars in addition to the HTS current leads.

The present report describes the CRPP contribution to the EFDA Task TW4-TMSF-HTSCOM. The comparison of the actual ITER design with and without HTS current leads will be presented in a separate final report prepared by the Forschungszentrum Karlsruhe.

The close collaboration of CRPP and the Forschungszentrum Karlsruhe within the frame of the present task is reflected by the fact that both associations have contributed to each of the two sub-tasks.

1. Introduction

The Centre de Recherches en Physique des Plasmas and the Forschungszentrum Karlsruhe were responsible for the development of a 70 kA current lead demonstrator for the International Thermonuclear Experimental Reactor (ITER). This work was performed in the framework of the European Fusion Technology Program. In the first half of 2004, the 70 kA HTS current lead was successfully tested in the TOSKA facility of the Forschungszentrum Karlsruhe [1-4]. In this test campaign, the heat exchanger part of the current lead was cooled by helium gas of 50 K inlet temperature. At the nominal HTS warm end temperature of 65 K the current lead could be safely operated in steady state at currents up to 80 kA. The nominal operating conditions (helium inlet temperature of 50 K, warm end HTS temperature of 65 K) have been selected based on the results of an optimization study [5], which indicates that the refrigerator input power needed to cool the current lead reaches a broad minimum close to these operating conditions. Because of an extremely large contact resistance of more than 40 nΩ the helium mass flow rate required to cool the heat exchanger part of the current lead was much higher than the design values.

In autumn 2004 the screw contact between the HTS and the heat exchanger part of the 70 kA current lead was filled with solder, leading to a considerably reduced contact resistance of less than 10 nΩ. After this modification the current lead was again tested in December 2004. Under these conditions the helium mass flow rates required to cool the heat exchanger part of the current lead were in good agreement with the design values [6].

From a system point of view it would be advantageous to cool the current leads with 80 K helium gas in parallel to the thermal shields. In spite of the fact that the 70 kA current lead was designed for a helium inlet temperature of 50 K and a HTS warm end temperature of 65 K it could be even operated using helium gas of 80 K inlet temperature. The resulting temperature at the warm end of the HTS part is close to 86 K [6]. These encouraging results clearly demonstrate that the HTS have reached the maturity that they can be used for the feeder system of ITER.

The new EFDA task TW4-TMSF-HTSCOM is again a joint work between the Centre de Recherches en Physique des Plasmas and the Forschungszentrum Karlsruhe. The primary objective of the task is the comparison of the actual ITER design with and without HTS current leads. This study will not only provide estimations of the differences in the investment and operating costs but also point out implications with other ITER components and the required ITER design changes. The performance assessment of HTS current leads for ITER is based on the test results of the 70 kA EU current lead. The work performed at the Forschungszentrum Karlsruhe is focused on this aspect.

A second objective of this task is the assessment of a third ITER design option, which not only replaces the conventional current leads but also the water-cooled aluminium bus bars by high-temperature superconductors. In addition to reduced electrical power losses, the use of HTS bus bars could provide significant savings in the space required for the installation. The work performed at CRPP concentrates on this option, which includes a conceptual design of HTS bus bars suitable for ITER. In addition to the feasibility of the HTS bus bars for ITER, economic aspects are considered. In the design of the HTS bus bars the originally considered nominal operating conditions for the 70 kA HTS current lead (helium inlet temperature of 50 K, HTS warm end temperature of 65 K) are used as a reference scenario. The possibility to operate the HTS bus bars using helium gas of 80 K inlet temperature has been also addressed.

As a basis for the present work the actual ITER feeder design has been reviewed. This design will be compared to the option using HTS current leads (see FZK final report) or HTS current leads and bus bars (this report). The overall performance of the different design options (1. Conventional current leads and water-cooled aluminium bus bars, 2. HTS current leads and water-cooled aluminium bus bars, 3. HTS current leads and HTS bus bars) is compared. The conceptual design of the HTS bus bars is described.

2. General Description of ITER

In this section, a general description of the ITER magnet system including the superconducting feeders and the normal conducting bus bars will be presented. Most of the content of this section has been deduced from different ITER documents [7-10].

2.1 General Description of the ITER Magnet System

ITER is an experimental fusion reactor according to the tokamak principle which for the first time will generate a plasma with power reactor-like properties over a longer time period (some 300 seconds). The investigations on plasma physics will concentrate on all aspects of a burning plasma which essentially is maintained by alpha-heating. Alpha heating means the transfer of kinetic energy of alpha particles originating from the fusion reaction to the plasma particles (electrons and ions).

Furthermore key technologies for a fusion power station (plasma heating, superconducting magnets, plasma facing components, fuel cycle and remote handling) will be tested under power reactor-like conditions. ITER is also capable to perform first tests of blanket concepts by suitable test modules. An artist view of ITER is shown in Figure 2-1.

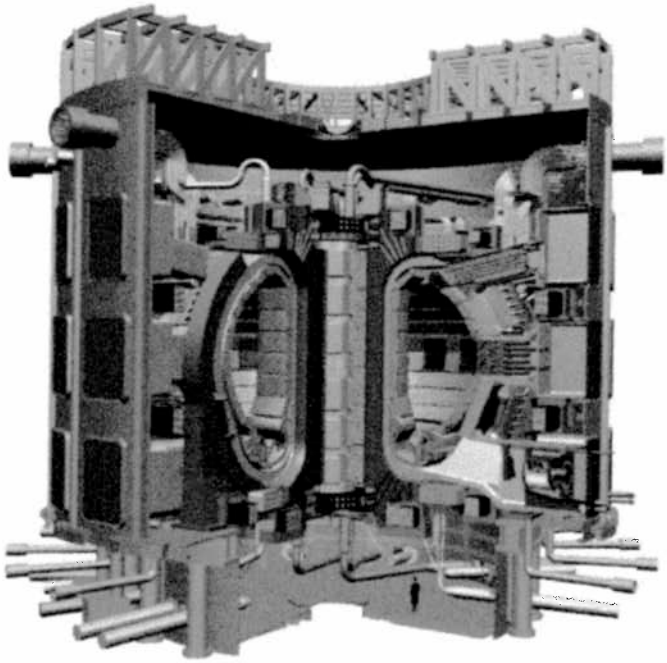

Figure 2-1. Artist view of ITER.

2.1.1 Magnet System

The magnet system for ITER consists of 18 toroidal field (TF) coils, a central solenoid (CS), six poloidal field (PF) coils and 18 correction coils (CCs). The magnet system elevation is shown on Figure 2-2.

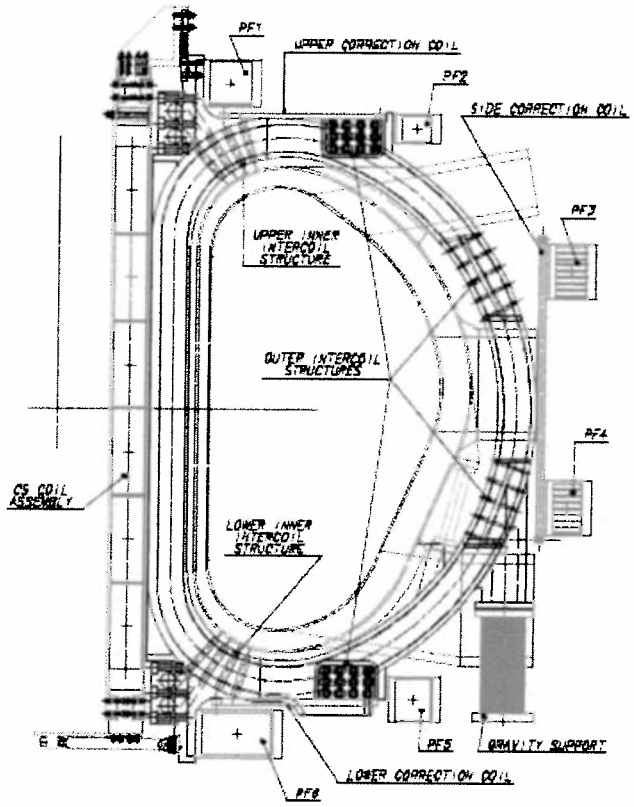

Figure 2-2. The ITER main magnet system

The TF coil cases, which enclose the TF coil winding packs, form the main structural component of the magnet system. The TF coil inboard legs are wedged all along their side walls in operation, with friction playing an important role in supporting the out-of-plane magnetic forces. In the curved regions above and below the inboard leg, the out-of-plane loads are supported by four upper and four lower poloidal shear keys arranged normal to the coil centreline. In these regions, the coils are linked by means of two upper and two lower pre-compression rings which provide a radial centripetal force and improve the operation of the shear keys. In the outboard region, the out-of-plane support is provided by four sets of outer intercoil structures (OISs) integrated with the TF coil cases and positioned around the perimeter within the constraints provided by the access ducts to the vacuum vessel. The OISs are structures acting as shear panels in combination with the TF coil cases. There is low voltage electrical insulation between TF coils in the inboard leg wedged region and between the OIS connecting elements in order to avoid the circulation of eddy currents.

The magnets are located within the cryostat which provides the thermal insulation for the 4.5 K superconducting coils from the ambient heat load. This is done by a vacuum within the cryostat to eliminate the convective heat loads, and by the use of intermediate thermal shields at 80 K to intercept the bulk of the thermal radiation and conduction from the cryostat and the vacuum vessel.

Feeders to the coils include the superconducting bus bars, cryogen service lines, and instrumentation cables. These feeders run from individual coil terminals inside the cryostat, through cryostat feedthroughs (CF) and into coil terminal boxes (CTBs) or structure cooling valve boxes (SCVBs). These boxes are located outside the cryostat and bioshield, in the tokamak galleries which are accessible for hands-on maintenance. The interfaces between the

magnet system and the power supplies and the cryoplant are at these boxes. Figure 2-2 shows a schematic view of the ITER main magnet system (TF, CS, PF).

2.1.2 Power Supplies

The interface between power supplies and the magnets occurs at the CTBs where the transition is made from superconducting bus bars to room temperature (water-cooled aluminium) bus bars. The power supplies have two physical interfaces to the magnets.

i) The current supplies and discharge circuits for the coils. These consist of one supply for the 18 TF coils plus 9 discharge resistors connected between each pair of coils. Each PF and CS coil module has its own supply and discharge resistor.

ii) The magnet structure grounding scheme. The magnet structures are all connected to ground through the bus bar containment pipes to the cryostat wall. The connection of the cryostat into the overall machine grounding scheme is part of the power supplies.

2.1.3 Cryoplant

The boundary between the cryoplant system and the magnet helium manifolding occurs at the CTBs and SCVBs. These boxes contain the adjustable valves that allow the proper distribution of the helium flow into the magnet components.

In operation, the cryoplant provides supercritical helium to the four sets of coils (TF, CS, PF and CCs), their superconducting bus bars, and the magnet structures. The coils, bus bars and structure cooling systems are subdivided into a number of closed loops where supercritical helium is circulated by a pump and re-cooled through a primary heat exchanger located in the auxiliary cold boxes of the cryoplant. For the coils, the supercritical helium is supplied in the temperature range of 4.4 - 4.7 K. The cryoplant also supplies liquid helium to the current leads and receives back gaseous helium at room temperature from these current leads.

2.2 Description of the ITER Superconducting Feeder System Layout

The superconducting current feeder system connects the magnets systems of ITER with the power supplies via current leads and superconducting bus bars. It mainly consists of superconducting (sc) bus bars, a sc bus line interface terminal (so-called coil terminal box (CTB)) and the current leads. These current leads will be either conventional or high temperature superconductor (HTS) type. Each sc feeder has a length of approximately 25 m and is made of three parts, the in-cryostat feeders, the Cryostat Feedthrough (CF) (including a straight section and an S-bend structure) and the CTB. This integrated system will be used as the current transmission system for the ITER magnet system. As the maximum field acting on the sc feeder is low and due to its complex cable structure, it has been decided to use similar kind of cable-in-conduit conductors for all the TF, PF and CS sc feeders which are made from NbTi / Cu. These sc feeders will also be cooled with forced flow supercritical Helium at 6 bar and 4.5 K as performed for the ITER magnets.

Each in-cryostat feeder is a subassembly that connects a coil or structure to the end of a Cryostat Feedthrough (CF) located just inside the cryostat; each has a robust steel outer

containment that provides protection to the cryostat components in the event of a short within the current supply bus bars. For a coil, it consists of the feed and return current supply bus bars (using NbTi superconductor), the return and supply helium lines and instrumentation lines. For the structures, the feeders contain a bundle of cooling pipes (since control of the supply to each of the 3 TF case cooling circuits is required). The upper structural feeders contain the 3 outlet supplies from the inside of the case as well as the outer surface outlets. The lower structural feeders contain a common inlet supply for each coil for all 3 circuits [11].

The CF includes a straight length from the cryostat wall to an S-Bend Box, as shown in Figure 2-3. In Figure 2-4, a cross-section of the feeder is shown.

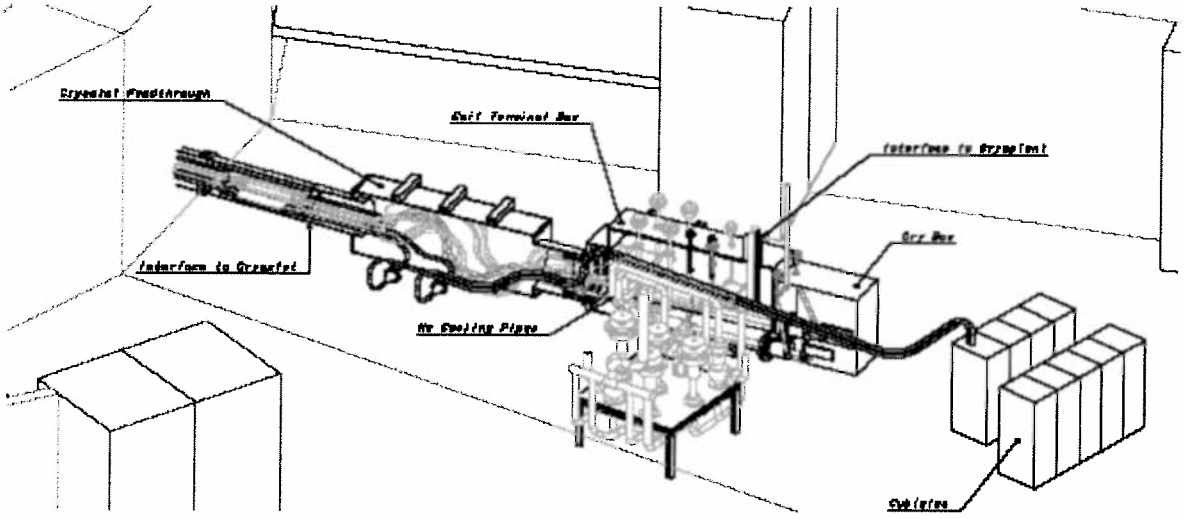

Figure 2-3. Schematic view of the cryostat feedthrough with S-bend and the CTB.

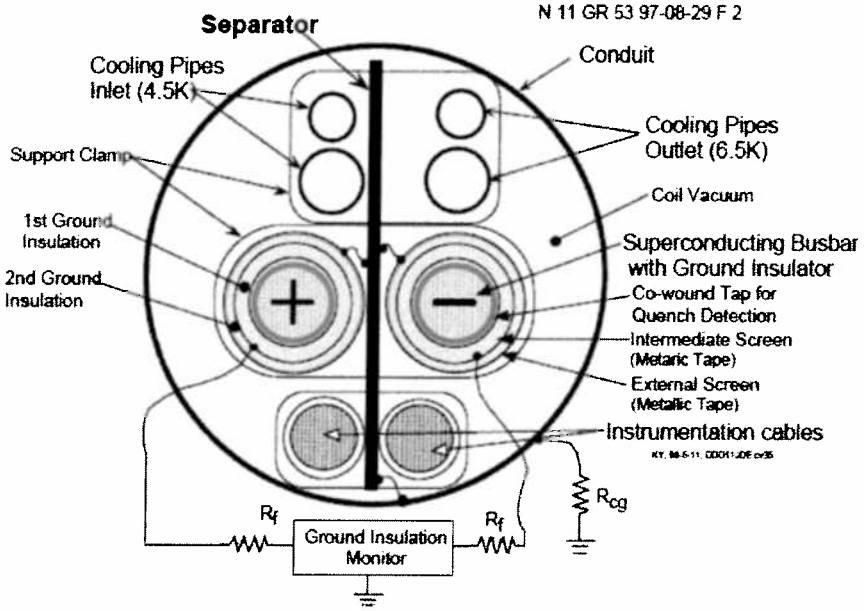

Figure 2-4. Cross section of the feeder.

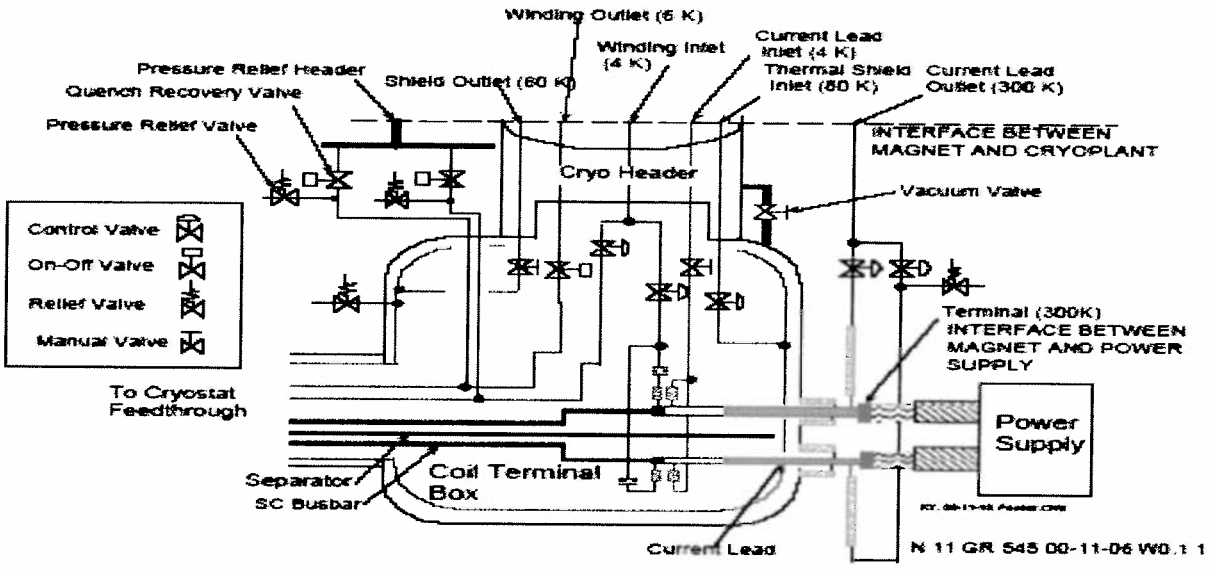

Figure 2-5. Cryogenic distribution within the CTB.

The S-bend box is also part of the CF and contains S-shaped bends in the bus bars and the cooling lines. These bends accommodate the movements of the in-cryostat feeders and the coils, relative to the fixed S-bend box and Coil Terminal Boxes (CTB), due to differential thermal contraction and expansion, electromagnetic forces, and earthquakes. The CTB consists of a pair of current leads along with the cryogenic distribution scheme as shown in Figure 2-5.

2.3 Coil Power Supply and Distribution

2.3.1 Design Requirements and System Description

The basic components of the Switching Network and Discharge Circuits are the Switching Network Units (SNUs) and the Fast Discharge Units (FDUs). Their function is to absorb the magnetic energy stored in the superconducting coils by inserting in series with the coils discharge resistors normally bridged by circuit breakers.

As already explained above, the ITER-FEAT magnet system consists of the eighteen TF coils (TF1-TF18), the Central Solenoid (CS), the six PF coils (PF1-PF6) and the nine Correction Coils (CCs). The CS is divided in two groups, symmetrical to the equatorial plane; each group consist of the 3 modules: CS1U, CS2U, CS3U (upper group) and CS1L, CS2L, CS3L (lower group). All TF coils are connected in series and are supplied by a common power source. The CS modules, PF coils and CCs are supplied by separate power circuits with exception of the CS1U and CS1L that are connected in series and powered by one power supply. Every individual Power Supply System (PSS) includes FDU(s) to protect the coils by the fast energy discharge in case of quenches. The SNUs are used in the PSS for the PF1, PF6 and all CS modules to generate the high voltage necessary for breakdown and plasma current initiation. The SNUs and FDUs are part of the coil power supply system DC circuits as well as the bus bars connecting the power supplies (thyristor converters) via the FDUs and SNUs with the

coil terminals. Table 2-1 shows some basic requirements mainly determined by the coil current and voltage design limitations.

Table 2-1. General requirement for DC components.

Parameter	Unit	TF	CS, PF1 & PF6	PF2 – PF5	Correction Coils
Maximum current	kA	68	45	45	7.5
Max. current duration	s	continuous	3800*	3800*	3800*
Short circuit current	kA	300	200	200	40
Max operating voltage	kV DC	10	10	14	1.0
Design insulation voltage between poles /contacts /terminals and to ground	kV AC	17.5	17.5	17.5	3.3

*- Duty factor varies in the range of 0.3 -0.7 depending on the cycle duration.

The fast discharge will be initiated if a quench occurs in one of the superconducting coils or in case of a very serious fault in the power supplies that can cause damage to the coils. It is assumed that the total number of the fast discharges during the life-time of the machine will not exceed 100 for the TF coils and 500 for the CS and PF coils. Therefore, the DC circuit breakers that will be used for the coil fast discharge shall be designed for at least 50 operations without replacement of sacrificial contacts and a few hundreds operation without major maintenance. Specific requirements for the FDUs are given in Table 2-2.

Table 2-2. FDU design requirements.

Parameter	Unit	TF	CS3U	CS2U	CS1	CS2L	CS3L
Number of FD Units		9	1	1	2	1	1
Max energy to be dissipated (per FDU)	GJ	3.82	1.15	1.2	1.2	1.2	1.15
Fast discharge time constant	s	11	7	7	7	7	7
		PF1	PF2	PF3	PF4	PF5	PF6
Number of FD Units		1	1	1	1	1	1
Max energy to be dissipated	GJ	1.0	0.42	1.9	1.6	1.6	2.10
Fast discharge time constant	s	14	14	14	14	14	14

Most of the Switching Network and Fast Discharge Circuit components, except for the TF FDUs, will be located in the Magnet Power Supply Switching Network Building. The switches of the TF FDUs will be placed in the Pit of the Tokamak Building, close to the Coil Terminal Boxes (CTBs); the discharge resistors and the counterpulse capacitors will be located in the adjacent building: Diagnostic Hall.

A description of the DC circuits including the FDUs, the SNUs, the element of the grounding system and other components is given in the following using as examples the TF and PF1 Power Supply Systems (PSSs).

The TF coils are combined in nine groups. All coils are connected in series; the connection within each group is made inside the cryostat. Therefore, only 9 pairs of the current leads

(half of the coil terminals number) are available outside the cryostat for connection to the switches initiating the fast discharge of the energy stored in the coils.
The nine FDUs are interleaved with the pairs of the series-connected coils. The FDUs consist of circuit breakers and discharge resistors. Two circuit breakers are included and connected in series in each of the FDUs. The first, called the current commutation unit (CCU), is designed for multiple operation and will open when a quench is detected. The second, explosively actuated circuit breaker (pyrobreaker, PB) is used as a backup, if the CCU has failed.

2.3.2 DC Bus Bars, Interconnections and Removable Links

The DC bus bars will connect the TF, CS, PF and Correction Coils to the AC/DC converters, the FDUs and the SNUs. Aluminium will be used as the material for all the bus bars.

All bus bars routed from the CTBs located in the pit in the Tokamak Building through the Galleries and Diagnostic Hall up to MPSSNB, will be water-cooled. Grounded cases and separators between "+" and "-" poles will be provided to protect the bus bars from damage and to decrease the probability of a pole-to-pole short circuit.

All the bus bars inside the MPSSNB and the MPCB, and on the bridges connecting these buildings will be air-cooled. The air-cooled bus bars will be provided, where possible, with protective cages and grounded separators. The connections between water-cooled and air-cooled bus bars will be made inside the MPSSNB.

2.3.2.1 Water-cooled bus bars and interconnections

The main design data on the water-cooled DC bus bars are given in Table 2-3.

Table 2-3. Design data of the water-cooled bus bars

Device / Parameter	Unit	TF	CS & PF	CC
Rated current	kA	68	45	10
Rated voltage (between poles and to ground)	kV AC	17.5	17.5	3.3
Short circuit current	kA	300	200	40
Cross-section	mm^2	41000	20000	4500
Total length *	m	100	1300	1000
Total number of flexible joints *		4	50	40
Total number of bends *		3	60	50

* refers to two-polarity bus bars

Examples of the designs of the water cooled bus bars and their flexible joints are shown in Fig. 2-6 and 2-7. The TF coils CTBs will be connected with the FDUs located nearby with the water-cooled interconnections of the same cross-section as the main bus bars (41000 mm^2). The length of one connection is 12 m including two bends (one on each end). Moreover, a flexible connection on each side should be provided. Total number of the one-polarity interconnections is 18.

2.3.2.2 Air-cooled bus bars and interconnections

The main design data of the air-cooled DC bus bars are given in Table 2-4.

Table 2-4. Design data of the air-cooled bus bars

Device / Parameter	Unit	TF	CS & PF	CC
Rated current	kA	68	45	10
Rated voltage (between poles and to ground)	kV AC	17.5	17.5	3.3
Short circuit current	kA	300	200	40
Cross-section	mm^2	72000	32000	7200
Total length *	m	150	2100	3000
Total number of flexible joints *		3	40	60
Total number of bends *		2	40	40

* - refers to 2 - polarity bus bars

The relatively short interconnections between the main bus bars and the PF FDU and SNU components (switches) will be made with the copper, 24 000 mm^2, bus bars. The total length of these bus bars is approximately 750 m.

2.3.2.3 DC links

These links provide flexibility during the commissioning period. In every individual PSS they provide a closed circuit that includes one AC/DC converter, the FDU(s) and a dummy load. In the CS & PF systems the SNUs can be also included in this circuit (together with the FDU or separately). The coils will be excluded in this circuit with the help of disconnector (in CS/PF PSSs) or links (in the TF system). The links in the CS/PF systems should be designed for the 20 s ON/20 s OFF operation under the maximum rated current (45 kA). The average length of these links will be about 1 m; the total number is 44. The links for bypassing the TF coils will have the same design as the 10 kA bus bars for the CC system: 4500 mm^2, water-cooled bus bars. Nine links of 30 m each will be used for this purpose.

Current reversing links will be used to change polarity of the AC/DC converters in the TF PSS and of the SNUs in the CS/PF PSSs if the plasma current direction has to be changed (see drawings N41GR 227 and 228). These links should have the same ratings as the main bus bars. The total number of the 1 m (in average) links will be 4 in the TF and 36 in the CS/PF PSSs.

2.3.2.4 ITER design of water-cooled aluminium bus bars

Tables 2-5 and 2-6 show the main parameters of the TF and CS&PF water-cooled bus bars. The maximum unit length is 10 m from which it can be seen that there are a lot interconnections and bendings on the way from the CTB and the FDU respectively to the

SNU. Another parameter which will be a challenge for HTS bus bars is the short circuit current of 300/200 kA for at least 100 ms where no quench will occur.

Table 2-5. TF PS water-cooled bus bars [9]

Table number: 41D4-10	Title: TF PS Water-cooled Busbars		
Reference number in Equipment List: 41D-4.6.1.1, 41D-4.6.1.2	Reference drawings: 41GR 118, 41GR 119, 41GR 125	Originator: RF HT	
Data category	Parameter	Value	Value
GENERALS	Function	DCbusbar	DCbusbar
	Type of busbar	single	double
	Applicable IEC standards	IEC 694	IEC 694
	Conductor material	aluminium ASTM6063	
	Insulation material	micoglass	micoglass
	Separator material	Glass-cloth-based laminate	Glass-cloth-based laminate
	Case material	steel	steel
	Cross section of conductor, mm^2	41,000	2x41,000
	Rated voltage, kV	24 AC	24 AC
	Rated operating current, kA	68	68
	Short circuit current/duration, kA/ms	300/100	300/100
	Rated peak withstand current, kA	300	300
	Maximum operating temperature, °C: continuous operat. short circuit operat.	60 95	60 95
BUSBAR DATA	Current density, A/mm^2	1.66	1.66
	Busbar shape, mm	4x(112x112)	2x[4x(112x112)]
	Busbar dimensions, mm	425x425	425x690
	Minimum bending radius, mm	see dr. 41GR 125	see dr. 41GR 125
	Safety margin of mechanical stress design, MPa	75	75
	Resonant frequencies		
STRAY PARAM.	DC resistance, mΩ/m at room temperature at continuous operating temperature	0.72 0.85	1.44 1.7
	Stray inductance for straight installation, μH/m	1	1
	Stray capacitance, pF/m between poles/to ground		
INSULATION	Rated insul. level according to ground IEC 71, kV between terminals	24 AC 24 AC	24 AC 24 AC
ENDURANCE	Life time, years	15	15
COOLING	Cooling system	water	water
	Max. power to be dissipated in the cooling water, kW/m	3.9	7.8
	Maximum power to be dissipated in the room air, kW/m	0.4	0.8
	Demineralised water: maximum conductivity, μS/m maximum inlet temper., °C maximum outlet temper., °C water flow, m^3/h per m maximum inlet pressure, MPa maximum pressure drop, MPa	100 45 60 0.23 0.5 0.25	100 45 60 0.46 0.5 0.25
	Maximum operating time without forced cooling (water flow = 0%) at rated operating current, s	1,750	1,750
AMBIENT CONDITIONS	Location	indoor	indoor
	Maximum earthquake withstand acceleration, g horizontal/vertical	0.2/0.2	0.2/0.2
SIZES AND WEIGHTS	Total layout cross section, mm: WxH	425x425	690x425
	Total weight (aluminium) kg/m	111	222
	Weight of the heaviest piece in shipping configuration, kg	1,400	2,500
	Weight of the heaviest piece to be handled during installation, kg	1,400	2,500
	Sizes of the largest piece, m, LxWxH	10x0.425x0.425	10x0.69x0.425

Table 2-6. CS&PF PS water-cooled bus bars [9]

Table number: 41D4-11	Title: CS & PF PS Water-cooled Busbars	
Reference number in Equipment List: 41D-4.6.2.1	Reference drawings: GR 119, 41GR 125	Originator: RF HT

Data category	Parameter	Value
GENERALS	Function	DC busbar
	Type of busbar	double
	Applicable IEC standards	IEC 694
	Conductor material	aluminium ASTM6063
	Insulation material	micoglass
	Cross section of conductor, mm^2	2x20,000
	Rated voltage, kV	24 AC
	Rated operating continuous current	45
	Short circuit current duration, kA/ms	300/100
	Rated peak withstand current, kA	300
	Max. operating temper., °C continuous operat. short circuit operat.	60 95
BUSBAR DATA	Current density, A/mm^2	2.25
	Busbar shape, mm	2x[2x(156x78)]
	Busbar dimensions, mm	195x390
	Minimum bending radius	See draw.41GR125
	Safety margin of mechanical stress design, MPa	75
	Resonant frequencies	
STRAY PARAM.	DC resistance, mΩ/m at room/operating temperature	2.97/3.49
	Stray inductance for straight installation, μH/m	1
	Stray capacitance between poles/to ground	
INSULATION	Rated insul. level according IEC 71, kV to ground between terminals	24 AC 24 AC
ENDURANCE	Life time, years	15
COOLING	Cooling system	water
	Max. power to be dissipated in the cooling water, kW/m	7.06
	Max. power to be dissipated in the room air, kW/m	0.3
	Demineral. water: max. conductivity, μS*m max. inlet temperature, °C max. outlet temperature, °C water flow, m^3/h per m max./min. inlet pressure, MPa max. pressure drop, MPa	100 45 60 0.2 0.5/0.1 0.21
	Cool down time from max. temperature without load current	
	Max. operating time without forced cooling at rated current, s	800
AMBIENT CONDITIONS	Location	indoor
	Max.earthquake withstand acceleration, g horizontal/vertical	0.2/0.2
SIZES AND WEIGHTS	Total layout cross section, mm W x H	345x540
	Total weight (aluminium) kg/m	108
	Weight of the heaviest piece in shipping configuration	1,300
	Weight of the heaviest piece to be handled during installation	1,300
	Sizes of the largest piece, mm LxWxH	10,000x345x540

Figures 2-6, 2-7 and 2.8 show the layouts of the water-cooled aluminium bus bars.

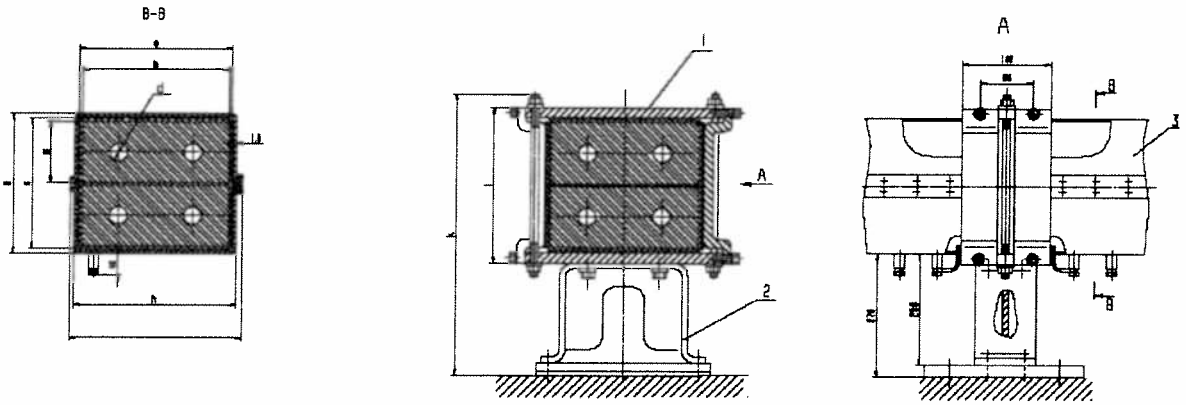

I, kA	a, mm	b, mm	c, mm	d, mm	e, mm	g, mm	h, mm	i, mm	m, mm	l, mm	k, mm
68kA	107	200	229	25	210	236	217	221	280	260	520
45kA	53	200	121	20	210	128	217	221	280	152	412

Figure 2-6. Layout of the single water-cooled aluminium bus bars.

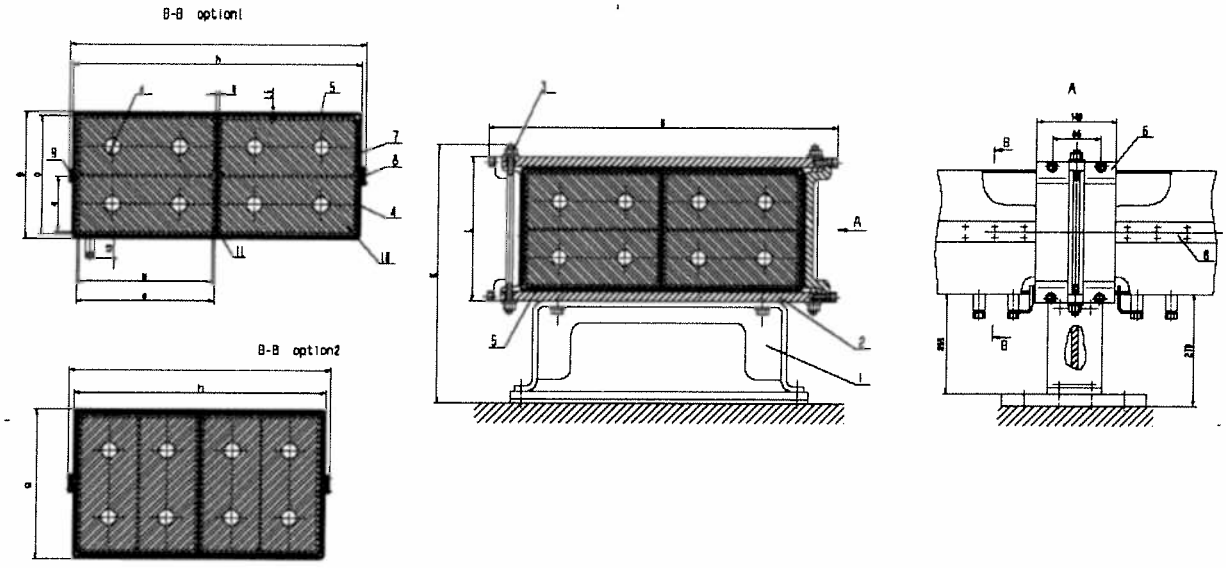

I, kA	Dimensions, mm	a	b	c	d	e	g	h		m	l	k
68	Basic option	107	200	229	25	210	236	452	456	500	260	520
45	Option 1(basic)	53	200	121	20	210	128	452	456	500	152	412
	Option 2						217	250	254			

Position	Component	Quantity	Remarks
1	Support	1	
2	Piece	2	
3	Wall	2	
4	Lower cover	1	
5	Beam	2	
6	Plate	2	
7	Upper cover	1	
8	Bolt M16	1	
9	Bolt M16	1	

Figure 2-7. Layout of the double water-cooled aluminium bus bars.

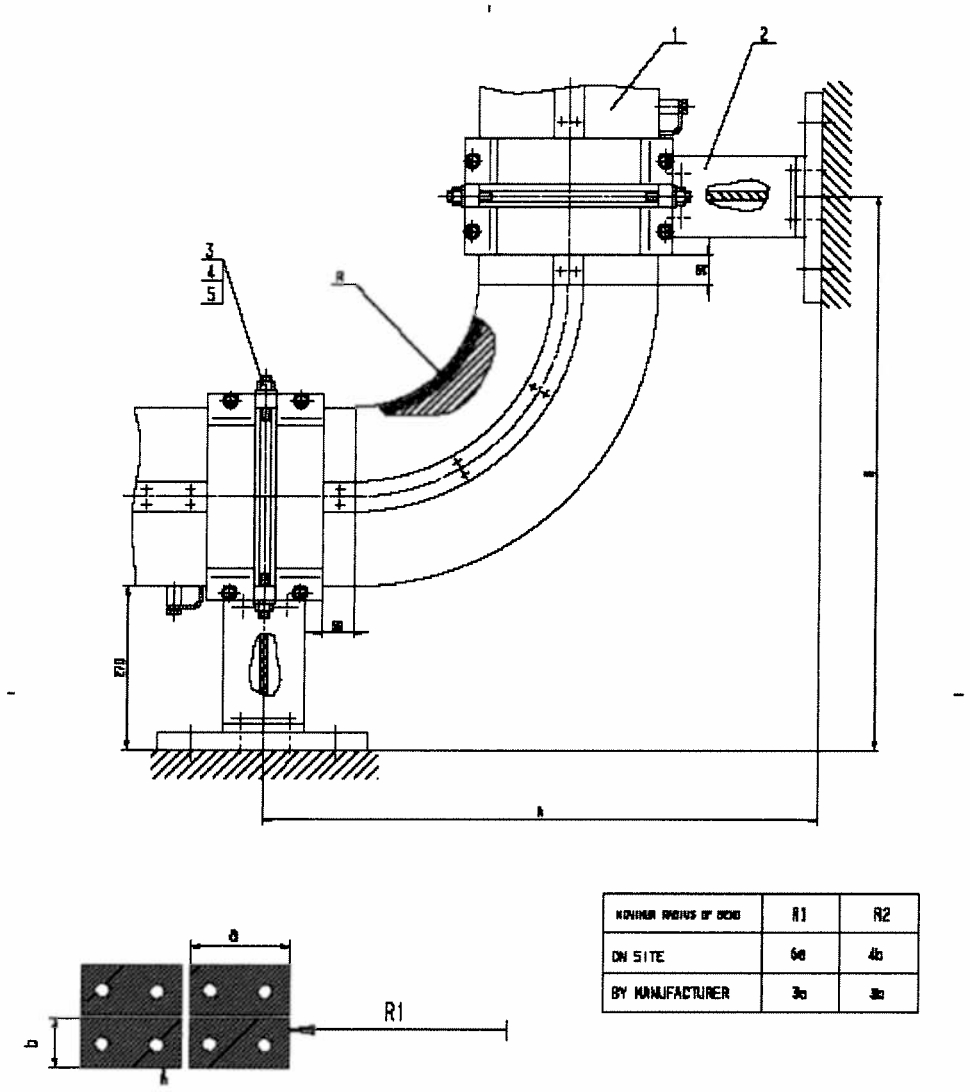

	R1	R2
ON SITE	6a	4b
BY MANUFACTURER	3a	3a

Figure 2-8. Layout of the bending of water-cooled aluminium bus bars.

3. Comparative Studies of Current Lead Performances

3.1 Introduction

The objective of the present report is an ITER design option using both HTS current leads and HTS bus bars. The aspects related to the use of HTS current leads instead of conventional ones is described in detail in the final report of the Forschungszentrum Karlsruhe. For a better readability the present ITER current lead design and the main results of the subtask performed at the Forschungszentrum Karlsruhe [12] are also briefly described in the present report.

3.2 Present ITER Design

The following description has been taken from the ITER-DDD 1.1 [10]. Each CTB contains one pair of copper current leads, those for the CC contain 2 pairs. The helium cooled current leads provide electrical connection between the room temperature bus bars from the power supply and the superconducting bus bars at 4 K inside the CTB.

The base cryoplant load and space requirements for the current leads have been calculated assuming cooling with forced flow supercritical helium at 4.5 K inlet temperature, and without the use of either low temperature or high temperature superconducting inserts along the thermal gradient part of the lead. Improvements to the base design can be made at the time of procurement, as long as the alternative is fully qualified (i.e. has been manufactured and tested) and meets the base design requirements listed at the end of this section.

The number and capacity of the current leads are listed in Table 3-1. A sketch of the conceptual design is shown in Figure 3-1.

Table 3-1. Current leads requirement for ITER

Coil type	No. of Coils	No. of current lead pairs	Max. current	Operation
TF	18	9	68 kA	Steady state
PF	6	6	52 kA	Pulsed
CS	6	6	45 kA	Pulsed
CC	6/6/6	9	10 kA	Pulsed

The current scenarios for the CS, PF and CC are pulsed, and in some plasma scenarios the coils are operating well below their maximum design values for most of the time (i.e. during the dwell and burn phases). A current lead designed to work efficiently at maximum current will generally not work at optimum performance at lower currents (generally, the extra copper needed to reduce the resistive heating at high current produces extra heat conduction from the warm end at lower currents). At present this has not been included in the design considerations but could be a factor in later optimization. The current leads are sized for optimum performance when carrying the coil maximum design current. The helium flow to the leads is not adjusted to follow the operating current through a pulse scenario (although it

could be reduced for the PF, CC and CS for periods when there is no plasma operation). It could be set too low for the peak operating current, so that the lead operates in a transient condition, with a slow (time scale many hundreds of seconds) when the current exceeds the design current, and a slow recovery when it is less.

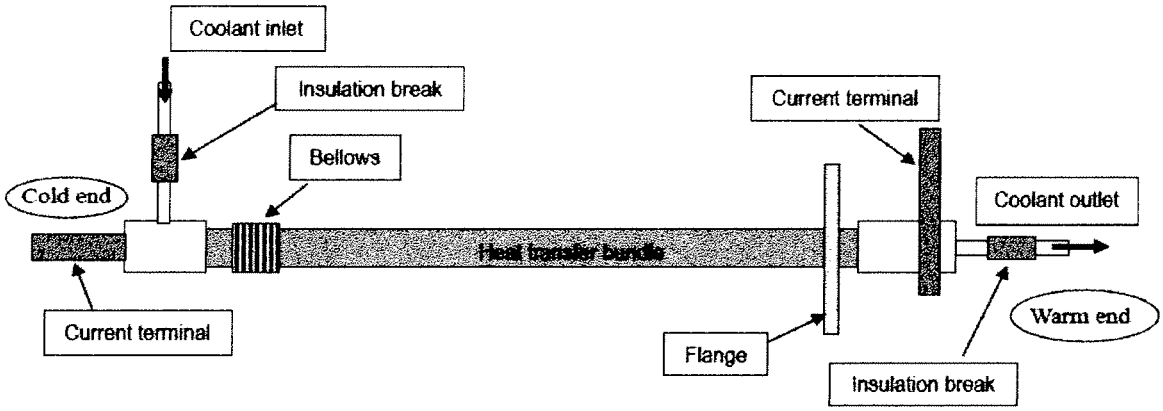

Figure 3-1. Schematic diagram of the forced flow conventional current lead design.

A further design consideration is operation under faulted conditions. For a current lead, the most serious condition is a loss of helium flow. For ITER, it is essential that even under these conditions the current leads can continue to operate for a time much longer than that required to detect the loss of flow and discharge the coils. Two conditions are adopted for a complete loss of flow

1) That the time taken for the temperature of the hot end to rise by 100 K is > 300 s (to give time for detection)

2) That the heat load at the cold end to the conductor increase by less than a factor of 3 in 600 s

3.3 Power Consumption Calculation [12]

For evaluation of the operational costs the efficiency of the specific refrigerator system plays a key role. In [13], approximations have been used to compare the operation costs of a HTS current lead to a conventional one.

Here, the power consumption is calculated using the following relation:

$$P_g = (dm/dt)(H_r/e_1) + Q_k(P_e/P_k)_{refrigeration} = (dm/dt)(H_r/e_1) + Q_k/(\eta_C\, e_2) \qquad (1)$$

Where

dm/dt = mass flow rate of coolant in (g/s),
Q_K = conduction and resistive loss at cold end, i.e. at 4.5 K level
H_r = 300 $(S_1 - S_2) - (h_1 - h_2)$ = 5919 J/g for 300 K to 4.5 K at 5 bar pressure.
η_C is the Carnot efficiency of the machine, = $[T_c / (T_w - T_c)]$

e_1 is the thermodynamic efficiency at different temperatures
e_2 is the thermodynamic efficiency at 4.5 K

It is assumed that the efficiency factors e_1 and e_2 reach a value of 29.5 % at 4.5 K. These efficiency factors depend upon the particular refrigeration system and its capacity.

3.4 Forced Flow Cooled Conventional Current Leads [12]

For constant cross section conventional leads, the following performance data are used:

$\dot{m}\,(I = 0) = 0.04$ g/s/kA/lead

$\dot{m}\ (I = I_{max}) = 0.06$ g/s/kA/lead

$Q_K\,(I = 0) = 0.1$ W/kA/lead (Conduction loss at cold end)

$Q_K\,(I = I_{max}) = 0.1$ W/kA/lead + $I_{max}^2\,R_j$ with $R_j = 1$ nΩ

Efficiency factor $e_1 = e_2 = 29.5$ % at 4.5 K

The main operating conditions and the refrigerator input power required by conventional current leads are summarized in Table 3-2.

Table 3-2. Operating conditions and the refrigerator input power required by a single conventional ITER current lead at the maximum current.

System	I_{max} (kA)	Number of CL	$\dot{m}\,(I_{max})$ (g/s)	$\dot{m}\,(I=0)$ (g/s)	$Q_k(I_{max})$ (W)	$Q_k(I=0)$ (W)	$\dot{m}\,H_r/e_1$ (kW)	$Q_k(P_e/P_k)$ (kW)	P_g (kW)
TF	68	18	4.08	2.72	11.4	6.8	81.9	2.71	84.6
PF*	52	12	3.12	2.08	7.90	5.2	62.6	1.87	64.5
CS	45	12	2.70	1.80	6.53	4.5	54.2	1.55	55.7

* 45 kA in normal operating mode

3.5 HTS Current Leads [12]

The performance of the EU 70 kA HTS current lead is used to estimate the refrigerator input power required by ITER HTS current leads. The main test results regarding the performance of the EU 70 kA HTS current lead are listed in Table 3-3. The reduction factors in the needed refrigerator input power achievable by the use of HTS current leads are gathered in Table 3-4.

Table 3-3. Operating conditions and the refrigerator input power required by the 70 kA HTS current lead [12].

	Scenario 1		Scenario 2		Scenario 3	
I (kA)	0	68	0	68	0	68
T_{He}^{inlet} (K)	50	50	50	50	80	80
$\dot{m}_{He}$ (g/s)	2.17	4.7	1.0	4.7	1.51	15.0
T_{HTS}^{warm} (K)	65	65	105	65	105	85
Q_k^{cond} at 4.5 K (W)	13.5	13.5	24.0	13.5	24.0	18.9
Q_k^{Joule} at 4.5 K (W)	-	17.1		17.1		17.1
$\dot{m} H_r/e_1$ (kW)**	11.6	25.2	5.4	25.2	5.9	58.4
$Q_k(P_e/P_k)$ (kW)	3.2	7.2	5.7	7.2	5.7	8.5
P_g (kW)	14.8	32.4	11.1	32.4	11.6	66.9

** e_1 = 28.4 % , H_r = 1521 J/g (T_{He}^{inlet} = 50 K), e_1 = 25 % H_r = 973 J/g (T_{He}^{inlet} = 80 K), p = 4.4/4.6 bar

Table 3-4. Reduction factors in the refrigerator input power necessary to cool the current leads provided by the use of HTS [12].

	HTS CL T_{He}^{inlet} = 50 K T_{HTS}^{warm} = 65 K	HTS CL T_{He}^{inlet} = 50 K T_{HTS}^{warm} = 105/65 K	HTS CL T_{He}^{inlet} = 80 K T_{HTS}^{warm} ≅ 105/85 K	HTS CL T_{He}^{inlet} = 80 K T_{HTS}^{warm} ≅ 85 K Neglecting 80 K mass flow rate
Standby	3.79	5.11	4.89	9.91
Operation	2.66	2.66	1.27	10.66
ITER duty cycle*	3.39	4.08	2.79	9.97

* TF coils: 16/24 × 5/7 × 8/12 = 0.32 (16 h/day, 5 working days/week, 8 month of operation per year)
PF/CS coils: 3/24 × 5/7 × 8/12 = 0.06 (3 h/day operating time)

3.6 Economic Aspects of the Use of HTS Current Leads [12]

The use of binary HTS current leads can considerably reduce the cooling power needed for the current leads. The main results of the sub-task performed at the Forschungszentrum Karlsruhe are summarized below.

Required refrigerator input power for all ITER current leads:

Conventional current leads 2.164 MW

HTS current leads

a) T_{He}^{inlet} = 50 K, T_{HTS}^{warm} = 65 K 0.638 MW
b) T_{He}^{inlet} = 50 K, T_{HTS}^{warm} = 105/65 K 0.530 MW
c) T_{He}^{inlet} = 80 K, T_{HTS}^{warm} = 85 K 0.777 MW
d) T_{He}^{inlet} = 80 K, T_{HTS}^{warm} = 85 K (only 4.5 K level) 0.217 MW

Supposing electricity costs of 0.05 €/kW h the operation costs for all ITER current leads are:

Conventional current leads	0.948 M€
HTS current leads	
a) T_{He}^{inlet} = 50 K, T_{HTS}^{warm} = 65 K	0.279 M€
b) T_{He}^{inlet} = 50 K, T_{HTS}^{warm} = 105/65 K	0.232 M€
c) T_{He}^{inlet} = 80 K, T_{HTS}^{warm} = 85 K	0.340 M€
d) T_{He}^{inlet} = 80 K, T_{HTS}^{warm} = 85 K (only 4.5 K level)	0.095 M€

The reduction of the operation costs is between 0.716 M€ (b) and 0.853 M€ (d).

Concerning the HTS modules required for ITER, about 3.8 M€ are required. To this number, additional design and development costs including the fabrication and cold test of one prototype HTS current lead has to be added.

The higher investment costs for the HTS current leads are more than compensated by the cost saving for the 4.5 K refrigerator plant. If looking to the liquefaction capacity required to cool all ITER leads, 143 g/s would be needed at 4.5 K which is equivalent to about 22 kW refrigeration capacity. A 22 kW cryo plant unit will require much higher investment costs than the higher costs required for HTS current leads. Cost estimations for the cryo plant unit give about 10 M€ [12].

A final cost assessment can be made as soon as the parameters of the ITER cryo plant and of the ITER operation cycle are finalized.

4. Conceptual Design of HTS Bus Bars for ITER

4.1 Introduction

In a collaboration of CRPP and the Forschungszentrum Karlsruhe the possibility to replace the water-cooled Al bus bars by high-temperature superconductors has been investigated. In the present report, the conceptual design of HTS bus bars for the TF, CS and PF coils of ITER is described. The design is based on the availability of 50 K helium gas and a bus bar warm end temperature of 65 K. According to the results of a previous study [5] these operating conditions provide a minimum refrigerator input power necessary to cool HTS current leads. In addition, the economic aspects related to the replacement of the conventional current leads and the Al bus bars by HTS current leads and HTS bus bars are discussed.

4.2 Short Description of the Al Bus Bars

The Al bus bars for the TF coils are designed for a rated current of 68 kA. The rated voltage between poles and to ground is 17.5 kV. The TF bus bars consist of two aluminium conductors, each 200 mm in width and 107 mm in thickness (see Figure 2-6). In both sub-conductors, two pipes, each 25 mm in diameter, are embedded for the required water cooling [14]. The maximum inlet temperature of the cooling water is limited to 45°C. The total aluminium cross-section of the TF bus bars is approximately 41000 mm^2. The length of a single TF bus bar is 12 m. The minimum tolerable bending radii (on site bending) vary

between 428 and 1200 mm, depending on whether the thicker or the thinner side of the rectangular bus bar is bent. The duty factor for the steady state DC operation of the TF bus bars is 32 %.

The rated current of the PF and CS Al bus bars is 45 kA. In the case of the PF coils, a back-up mode with currents up to 52 kA is foreseen. The PF and the CS bus bars will be operated in pulsed mode. As in the case of the TF bus bars the rated voltage between poles and to ground is 17.5 kV. The PF and the CS bus bars are formed, similar to the TF bus bars, of two aluminium sub-conductors, each 200 mm wide and 53 mm thick (see Figure 2-6). The diameter of the cooling channels is 20 mm [14]. The total aluminium cross-section is approximately 20000 mm^2. The minimum tolerable bending radii (on site bending) vary between 212 and 1200 mm.

The electrical resistivity of aluminium is 3 _ 10^{-8} Ωm at an operating temperature of 50°C. The resulting resistance of the TF bus bars is 7.34 _ 10^{-7} Ω/m. At the rated current of 68 kA, a Joule heat of 3.4 kW/m is generated in the TF bus bars. The resistance of the PF and CS bus bars is 1.5 _ 10^{-6} Ωm leading to resistive losses of 3 kW/m at the nominal current of 45 kA. Because of the pulsed operation of the PF and CS magnet system, the root-mean-square (rms) values of the currents in the different coils are considerably smaller than 45 kA. The load factors based on the rms currents vary between 0.148 and 0.566 for the CS coils. The load factors for the PF coils are below 0.384 [15].

4.3 HTS Bus Bar Design

The design of the HTS bus bars is similar to that of superconducting power transmission cables. A sketch of a superconducting power transmission cable with a room temperature dielectric is shown in Figure 4-1. The superconducting Bi-2223 tapes are wound onto a flexible stainless steel former. For the DC operation of the TF bus bars, the current distribution among the layers is mainly determined by the contact resistances. In the case of the pulsed operation of the PF and CS bus bars, the inductive current distribution is of importance. In the development of superconducting power transmission cables it was found that for a constant twist pitch and alternating winding senses most of the AC current flows in the outermost layers of the cable. This behaviour is a consequence of the variation of the self and the mutual inductances of the different layers. A uniform current distribution among the layers can be achieved by variation of the twist pitches of the individual layers. In such a design the winding angle increases continuously from a negative minimum to a positive maximum value [16-18]. In the conceptual bus bar design presented in this report the aspect of optimised winding pitches will not be discussed.

The coolant flows in the space between the superconducting layers (outer radius r_{sc}) and the inner corrugated stainless steel pipe of the vacuum thermal insulation system (inner radius r_{1ith}, see Figure 4.2). Because of the constant number of Bi-2223 tapes in the different layers there exists a small gap between adjacent tapes in the outermost layers. If this space is not sufficient for the penetration of the cooling gas into the superconducting layers additional spacers may be introduced.

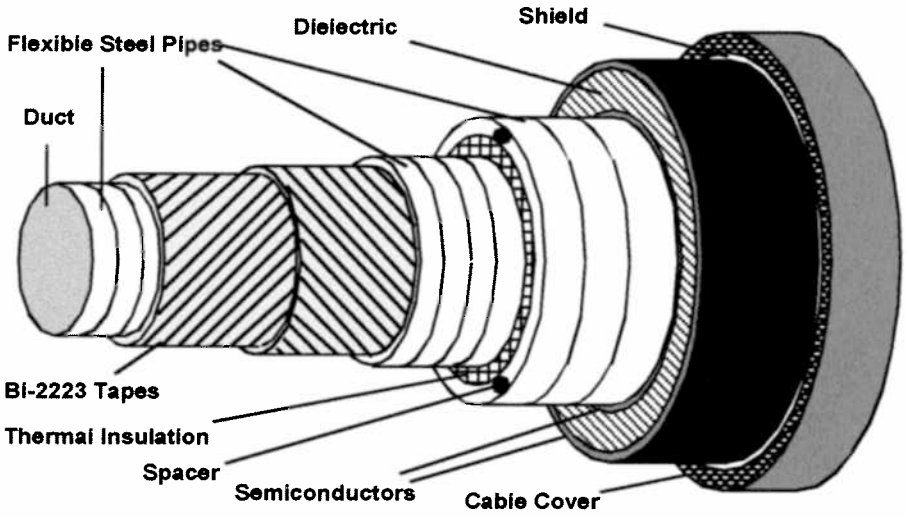

Figure 4-1. Schematic illustration of a single phase power transmission cable with warm dielectric.

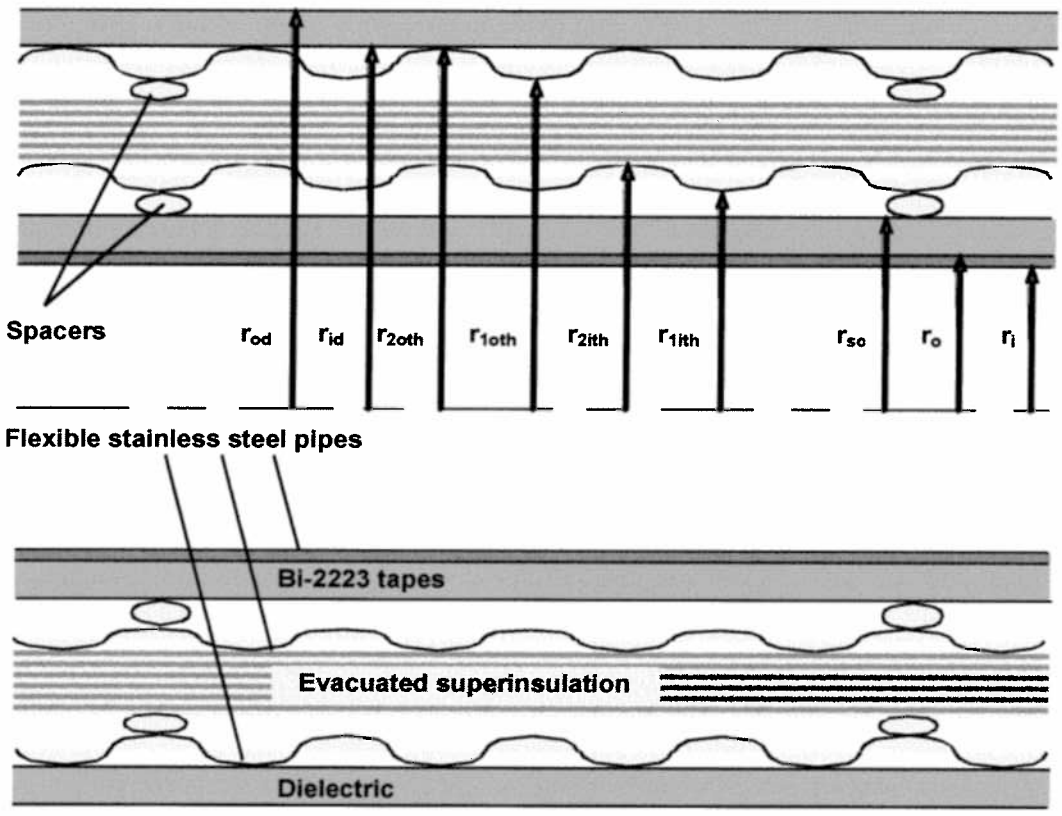

Figure 4-2. Sketch of a HTS bus bar for ITER showing the main dimensions needed for the design.

The main dimensions of a HTS bus bar are defined in Figure 4-2. The superconducting Ag/Bi-2223 tapes of 4 mm width and 0.22 mm thickness (dimensions of EAS standard Bi-2223 tapes) are wound onto a flexible stainless steel former of inner radius r_i and outer radius r_o. Due to the twist pitch the effective width w_{eff} of the Bi-2223 tapes is enlarged to a value $w/\cos\varphi$, where φ is the twist angle with respect to the axial direction. The number of tapes per layer is $n = U/w_{eff} = 2\pi r_o/w_{eff}$ (n is an integer number). The determination of the required number of Bi-2223 layers and the cable critical current is described in Section 4.3.1. The thermal insulation of the bus bar is provided by evacuated superinsulation, which is embedded between two flexible corrugated stainless steel pipes. The heat leak through the thermal insulation is

$$P_{th} = \frac{2\pi\, k(T_{out} - T_{op})}{\ln(r_{1oth}/r_{2ith})} \tag{2}$$

where $k = 2 \_ 10^{-4}$ W/mK is the thermal conductivity of the evacuated superinsulation. The temperatures at the outer (r_{1oth}) and inner radii (r_{2ith}) of the thermal insulation are T_{out} = 300 K and T_{op}.

The electrical insulation of the bus bar is provided by a dielectric surrounding the outer flexible stainless steel pipe of the thermal insulation. The maximum electric field in the dielectric is

$$E_m = \frac{1}{r_{id}} \frac{U}{\ln(r_{od}/r_{id})} \tag{3}$$

where U is the voltage, r_{id} the inner and r_{od} the outer radius of the dielectric.

The AC losses in the PF and CS bus bars have been estimated for the reference operating scenario [19]. The operating currents occurring in the CS and PF conductors during the reference scenario are listed in Tables 4-1 and 4-2, respectively. The largest variation in the currents (+39.9 kA to -45 kA) is foreseen for the CS coils CS1U and CS1L. Using the monoblock model, an upper limit of the transport current AC loss can be estimated. In a hollow cylinder the transport current loss per cycle is [20, 21]

$$P_{AC} = \frac{\mu_0 I_{c0}^2}{\pi\, t_{cycle}} \left\{ (1-\Gamma)\ln(1-\Gamma) + \Gamma - \frac{\Gamma^2}{2} \right\} \tag{4}$$

with

$$\Gamma = \frac{I_p}{I_{c0}} \tag{5}$$

where μ_0 is the permeability of free space, I_p the peak current and t_{cycle} = 1800 s the duration of a full cycle. $I_{c0} = \pi\, r_{sc}^2\, j_{ov}$ is the fictitious critical current, which would result from the overall critical current density j_{ov} in a solid cylinder of radius r_{sc} (r_{sc}: outer radius of the outermost superconducting layer). In the estimation of the transport current AC losses averaged over a full cycle of 1800 s length a peak current of ±45 kA was used.

Table 4-1. Currents in the CS conductors during the reference operating scenario [19].

Magnet	CS3U	CS2U	CS1U	CS1L	CS2L	CS3L
Time (s)	I (kA)					
0	39.9	39.9	39.9	39.9	39.9	39.9
1.6	35.9	34.7	35.7	35.7	32.4	35.9
4.61	33.2	31	25.8	25.8	29.1	34.6
7.82	30.8	27.6	20.8	20.8	26.2	33.3
11.38	28.4	24.2	16	16	23.2	32.1
15.24	26	20.8	11.7	11.7	20.3	30.8
19.52	23.6	17.4	7.4	7.4	17.3	29.6
24.17	21.2	14	3.3	3.3	14.4	28.3
29.37	18.9	10.6	-1.2	-1.2	11.4	27.1
35.25	13.6	8.9	-6.4	-6.4	8.4	24.9
42.12	8.4	7.2	-11.3	-11.3	4.7	22.6
49.26	6.7	5.5	-17.1	-17.1	2.9	20.4
56.21	4.6	2.6	-22.1	-22.1	0.5	18.2
63.22	3.5	-1.8	-26.5	-26.5	-3.3	17.3
72.55	1.7	-6.1	-31.5	-31.5	-6.8	15.4
100	-2.1	-16	-40.4	-40.4	-15.6	10.3
105	-2.3	-16.5	-39	-39	-15.7	9
110	-2.4	-16.8	-38.1	-38.1	-15.8	8.1
115	-2.4	-17	-37.5	-37.5	-15.9	7.4
120	-2.5	-17.2	-37.1	-37.1	-16.1	6.9
125	-2.5	-17.2	-37	-37	-16.2	6.6
130	-2.6	-17.3	-37.1	-37.1	-16.4	6.5
530	-3	-35	-44.9	-44.9	-32.1	1
546	-0.8	-36.8	-43.8	-43.8	-32.5	0.6
564	2.4	-38.9	-42.3	-42.3	-32.9	0.3
580	5.8	-40.8	-40.8	-40.8	-33.3	0.2
590	6.8	-42.6	-43.2	-43.2	-34.6	2.2
616.6	1.6	-41.4	-39.5	-39.5	-33.6	-1.4
647.4	-4.6	-37.7	-32.9	-32.9	-30.7	-5.4
668.3	-8.7	-33.9	-27.4	-27.4	-28.4	-8.1
689.1	-12.9	-26.6	-23.6	-23.6	-24.3	-10.9
710	-17	-17.8	-17.8	-17.8	-17.8	-13.6
720	-19.1	-18.2	-18.2	-18.2	-18.2	-16.4
900	0	0	0	0	0	0
1490	0	0	0	0	0	0
1790	39.9	39.9	39.9	39.9	39.9	39.9
1800	39.9	39.9	39.9	39.9	39.9	39.9

Table 4-2. Currents in the PF conductors during the reference operating scenario [19].

Magnet	PF1	PF2	PF3	PF4	PF5	PF6
Time (s)	I (kA)					
0	38.2	5.9	2.6	2.2	3.5	19.9
1.6	32.8	2.5	1.8	1.2	0.4	19.3
4.61	34	-9.9	1.5	1.8	-8.4	21.8
7.82	35.2	-17.9	4	-5.1	-7.5	24
11.38	36.4	-20.4	3	-8.4	-8.7	26.2
15.24	37.5	-21.9	1.2	-10.9	-10.9	28.4
19.52	38.7	-21	-2.8	-10.3	-15	30.6
24.17	39.9	-21.8	-5.9	-10.3	-19.3	32.8
29.37	41	-21.3	-9.8	-10.8	-23.1	35
35.25	39.8	-21.3	-12.5	-12.5	-25.4	36.5
42.12	38.6	-22.1	-15.2	-13.7	-27.8	38
49.26	35	-22.5	-17.7	-15.6	-29.1	38.6
56.21	33.3	-24.3	-19.5	-17.8	-30.2	39.1
63.22	31.5	-25.5	-21.8	-19.8	-31.6	39.7
72.55	29	-26.4	-24.1	-21.6	-33	40.1
100	21.6	-25.5	-29.3	-22.8	-37	41
105	21.6	-23.5	-31	-24.8	-35.9	40.7
110	21.7	-22.2	-32.2	-26	-35.1	40.6
115	21.7	-21.3	-33.1	-27	-34.6	40.4
120	21.7	-20.9	-33.7	-27.6	-34.2	40.4
125	21.7	-20.9	-34.1	-27.8	-34.1	40.3
130	21.7	-21.2	-34.2	-28	-34.1	40.3
530	6.9	-18.5	-35.9	-28.5	-34.6	34.9
546	6.9	-19.8	-32.8	-28.1	-33.9	33.6
564	7	-22.6	-28.6	-27.7	-33	32.1
580	7	-25.9	-24.5	-27.5	-32.2	30.8
590	9.6	-32.9	-20.2	-26	-33.2	30.5
616.6	2.9	-27.1	-16.8	-22.4	-25	20.5
647.4	-5.2	-20.1	-12	-17.7	-15.7	8.5
668.3	-10.6	-17.1	-8.8	-11.5	-12.9	0.5
689.1	-16	-11.6	-5.7	-7	-7.1	-7.5
710	-21.4	-3.7	-2.7	-2.7	-0.5	-15.5
720	-23.8	-3.7	-2.1	-2.3	0	-16.4
900	0	0	0	0	0	0
1490	0	0	0	0	0	0
1790	38.2	5.9	2.6	2.2	3.5	19.9
1800	38.2	5.9	2.6	2.2	3.5	19.9

4.3.1 Determination of the Bus Bar Critical Current

The estimation of the bus bar critical current is based on the I_c data for AgMg/Ag/Bi-2223 tapes presented on the home page of European Advanced Superconductors (EAS). In the present study a maximum conductor temperature of 65 K is considered. Furthermore, the possibility to operate the HTS bus bars at temperatures of 80 or 85 K has been considered. To estimate the bus bar critical current at 65, 80 and 85 K it was necessary to use scaling laws approximating the measured in-field I_c data.

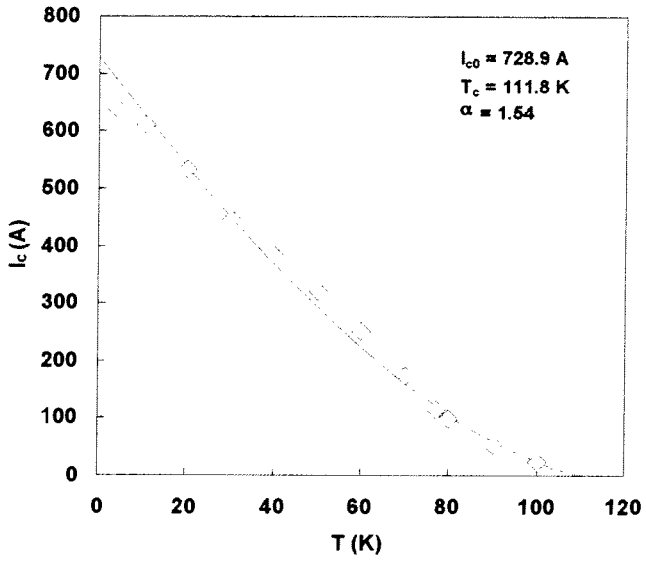

Figure 4-3. Critical current of AgMg/Ag/Bi-2223 tapes at zero applied field as a function of temperature.

The temperature dependence of the critical current of cuprate superconductors at zero applied field can be typically well represented by the scaling law [22]

$$I_c = I_{c0}\left(1-\frac{T}{T_c}\right)^{\alpha} \tag{6}$$

where I_{c0} is the critical current at zero temperature, T_c the critical temperature and α a scaling exponent. Figure 4-3 shows the critical current of the Bi-2223 tapes at zero applied field as a function of temperature. The solid line has been obtained from the scaling law (6). The values of the scaling parameters are:

$I_{c0} = 728.9$ A
$T_c = 111.8$ K
$\alpha = 1.54$

To reach high critical current densities in cuprate superconductors, a network of low-angle grain boundaries is required. In Bi-2223 tapes, a *c*-axis texture is sufficient to reach high critical current densities. This means that the crystallographic *c* axis of the superconducting filaments is perpendicular to the broad face of the tapes. Because of their layered structures the cuprate superconductors are characterised by highly anisotropic physical properties. Therefore, the field dependence of the critical current of the textured Bi-2223 tapes depends on the direction of the applied magnetic field with respect to the crystallographic *c* direction. The decrease of the critical current is more pronounced for magnetic fields parallel the crystallographic *c* axis, i.e. perpendicular to the broad face of the tapes. In the proposed bus bar design, the maximum magnetic field at the outermost Bi-2223 layer is parallel to the broad face of the tapes, which is the favourable field direction. Magnetic fields in the unfavourable field direction occur at conductor bends and are also generated by the return conductor.

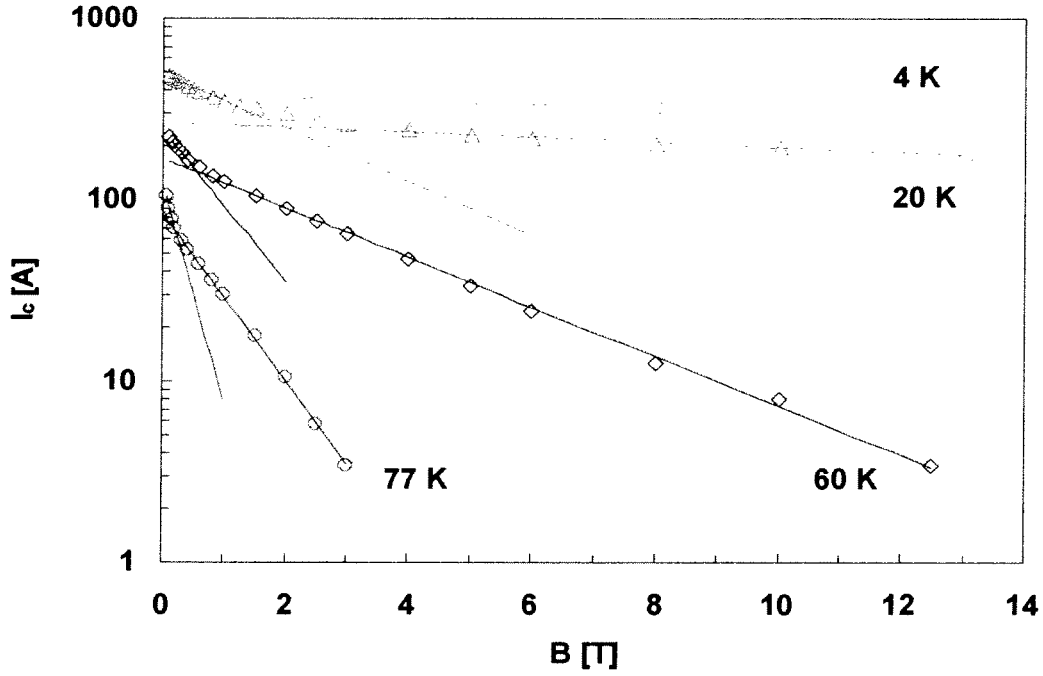

Figure 4-4. Critical current of Bi-2223 tapes as a function of the magnetic field parallel to the broad face of the tapes. The critical current of the tapes at 77 K in self field is 115 A.

Figure 4-4 shows the critical current of the Bi-2223 tapes as a function of the magnetic field applied parallel to the broad face of the tapes. The critical current decreases nearly exponentially with increasing applied field in the low and the high field region. The reciprocal values of the slopes of the straight lines can be considered as scaling fields. Generally, the scaling fields for the low field region are considerably smaller than those for the high field region.

The scaling fields for the high field region are shown in Figure 4-5. The data indicate that the scaling field for the high field region decreases exponentially with increasing temperature. The scaling temperature is much smaller than the critical temperature. Omitting the data point at 4 K a value of 16.37 K was found for the scaling temperature. The intersections of the high field trend lines and the current axis provide scaling currents $I_{sc}(T)$. These scaling currents as a function of temperature are shown in Figure 4-6 for fields parallel to the broad face of the tapes. The resulting scaling law for the critical current in the high field region is [22]

$$I_c(B,T) = I_{sc}(T)\exp\left(-\frac{B}{B_{sc}(T)}\right) \tag{7}$$

where the scaling parameters are defined as

$$B_{sc}(T) = B_{sc0}\exp\left(-\frac{T}{T_{sc}}\right) \tag{8}$$

$$I_{sc}(T) = I_{sc0}\left(1-\frac{T}{T_c}\right)^{\beta} \tag{9}$$

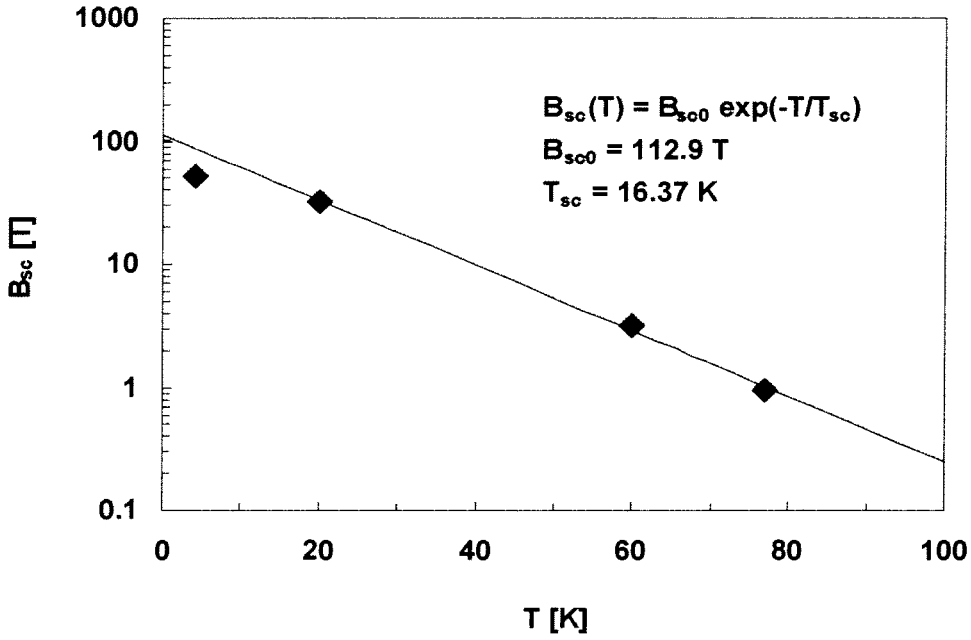

Figure 4-5. Scaling fields for high magnetic fields applied parallel to the broad face of the Bi-2223 tapes as a function of temperature.

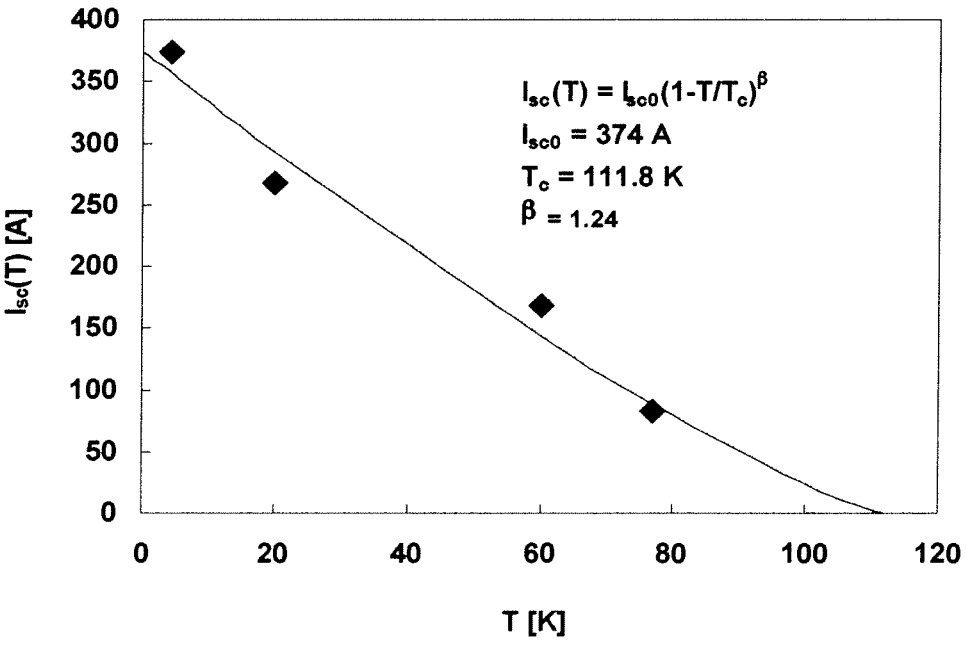

Figure 4-6. Scaling currents for high magnetic fields applied parallel to the broad face of the Bi-2223 tapes as a function of temperature.

The values of the scaling parameters for magnetic fields applied parallel or perpendicular to the broad face of the Bi-2223 tapes are given in Table 4-3.

Table 4-3. Scaling parameters used to describe the critical current of the Bi-2223 tapes in the high field region for fields applied parallel or perpendicular to the broad face of the tapes.

Scaling Parameter	Parallel Field	Perpendicular Field
T_c (K)	111.8	111.8
β	1.24	1.03
I_{sc0} (A)	374	250
B_{sc0} (T)	112.9	94.55
T_{sc} (K)	16.37	13.68

The critical current in low magnetic fields can be estimated using the following scaling relations.

$$I_c(B,T) = I_c(T,0)\exp\left(-\frac{B}{B_{sc}(T)}\right) \tag{10}$$

where $B_{sc}(T) = B_{sc0} - bT$ and $I_c(T, 0)$ is given by equation (6). The scaling parameters for the low field region are listed in Table 4-4.

Table 4-4. Scaling parameters used to describe the critical current of the Bi-2223 tapes in the low field region for fields applied parallel or perpendicular to the broad face of the tapes.

Scaling Parameter	Parallel Field	Perpendicular Field
B_{sc0} (T)	3.15	0.574
b (T/K)	0.0351	0.0062

Using equations (7) and (10) and the scaling parameters provided by Tables 4-3 and 4-4 the critical current can be estimated with an accuracy of 10-30 % in the region of interest. Figure 4-7 shows the critical current of the Bi-2223 tapes as a function of the magnetic field parallel to the broad face at a temperature of 65 K. The values have been calculated using the presented scaling laws.

In the present study the bus bar critical current has been determined for flexible stainless steel cable formers of 26.5, 34.0 and 42.25 mm outer radius. The number of Bi-2223 tapes in a single layer is 35, 46 and 57 for r_o values of 26.5, 34.0 and 42.25 mm, respectively. In the determination of the bus bar critical current the problem encountered is the fact that the maximum magnetic field generated at the surface of the outermost superconducting layer depends on the critical current of the Bi-2223 tapes, which is a function of the generated self field. The self-field generated by the multi-layer cable conductor is

$$B_s = \frac{\mu_0 n N I}{2\pi(r_o + Nt)} \tag{11}$$

where n is the number of Bi-2223 tapes per layer, N the number of layers, I the average current carried by a single tape, r_o the outer radius of the stainless steel former and $t = 0.22$ mm the thickness of a single Bi-2223 tape.

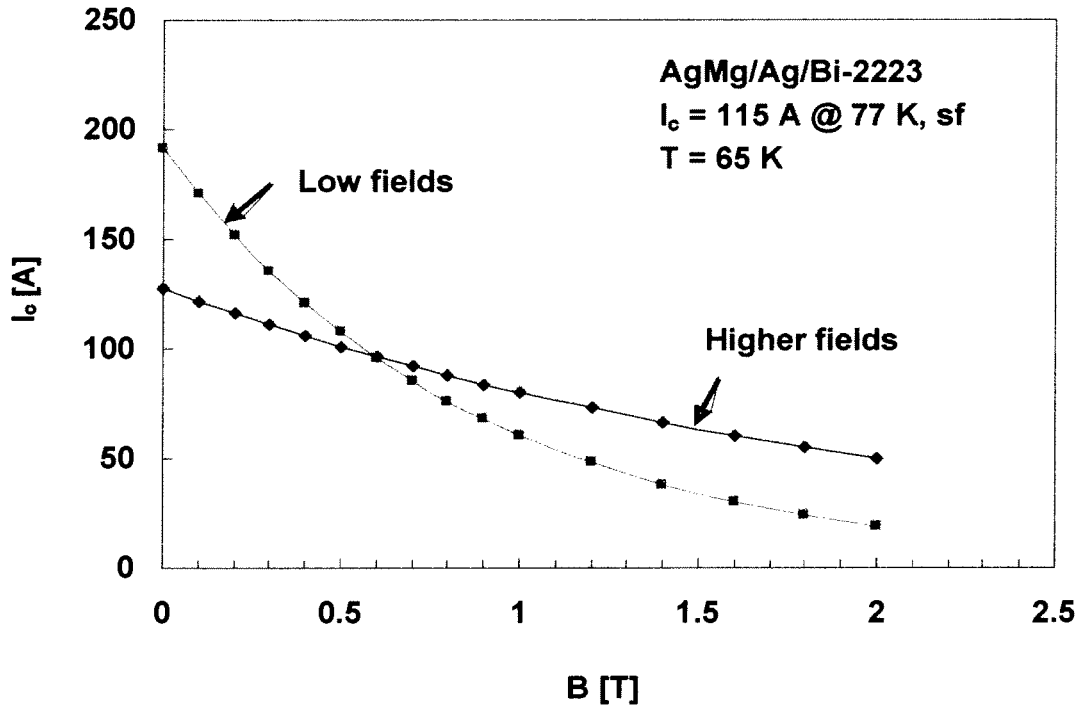

Figure 4-7. Critical current of AgMg/Ag/Bi-2223 tapes as a function of the magnetic field applied along the broad face of the tapes at 65 K.

At the bus bar critical current the tape current reaches $I_c(B_s)$, which leads to a bus bar critical current $I_c^{bb} = nNI_c(B_s)$. In Figure 4-8, the determination of the bus bar critical current is illustrated for a stainless steel former of 42.25 mm outer radius. In the considered example the number of Bi-2223 tapes per layer is 57. The intersections of the $I_c(B,T)$ line and the straight lines, describing the relation between the self-field and the tape current, provide the tape critical currents in the different multi-layer bus bars for an operating temperature of 65 K. For HTS bus bars with up to 16 layers of Bi-2223 tapes the self-field is in the region, where the tape critical current is well described by the low field scaling law (equations 6 and 10).

Using the results provided by design charts similar to Figure 4-8 for all considered former diameters, the bus bar critical current as a function of the number of Bi-2223 layers and the operating temperature has been determined. The bus bar critical currents at 65 K obtained for former diameters of 53, 68 and 84.5 mm are presented in Figures 4-9, 4-10 and 4-11, respectively.

The nominal operating current of the TF bus bars is 68 kA. To limit the ratio of the operating to the critical current to a value of 0.8 the minimum required critical current of the TF bus bars is 85 kA. The nominal operating current of the PF and CS bus bars is 45 kA. In the case of the PF bus bars a back-up mode with a conductor current of 52 kA is foreseen. To limit the value of I_{op}/I_c in the back-up mode to 0.8 a bus bar critical current in excess of 65 kA is needed. To avoid the necessity of a third bus bar design identical layouts are proposed for the PF and CS bus bars.

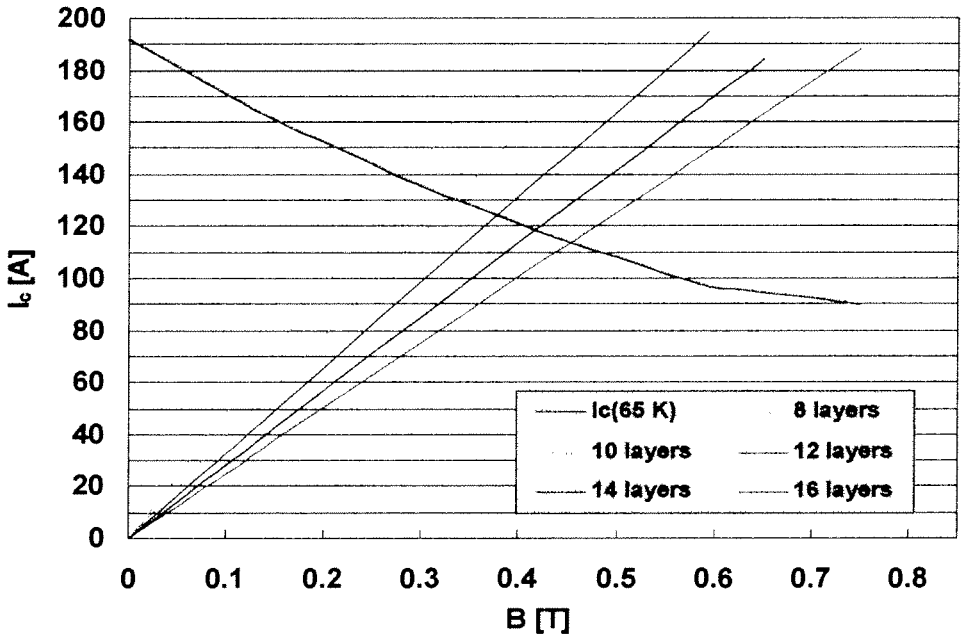

Figure 4-8. Determination of the critical current of Bi-2223 tapes in multilayer bus bars at 65 K. The Bi-2223 tapes are wound onto a flexible stainless steel pipe of 42.25 mm outer radius. The straight lines describe the relation between the tape current and the self-field at the outermost layer. The intersection of the $I_c(B,T)$ line and the straight lines provide the tape critical current at 65 K and the bus bar self-field.

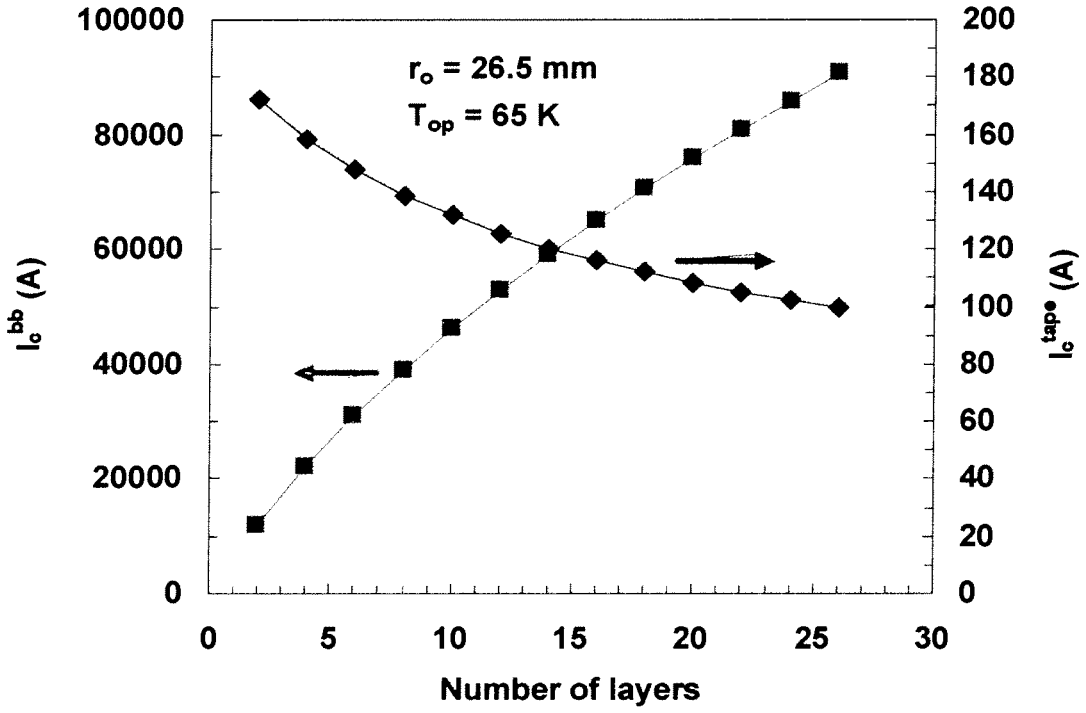

Figure 4-9. Bus bar and tape critical currents at 65 K as a function of the number of Bi-2223 layers wound onto a flexible stainless steel pipe of 26.5 mm outer radius.

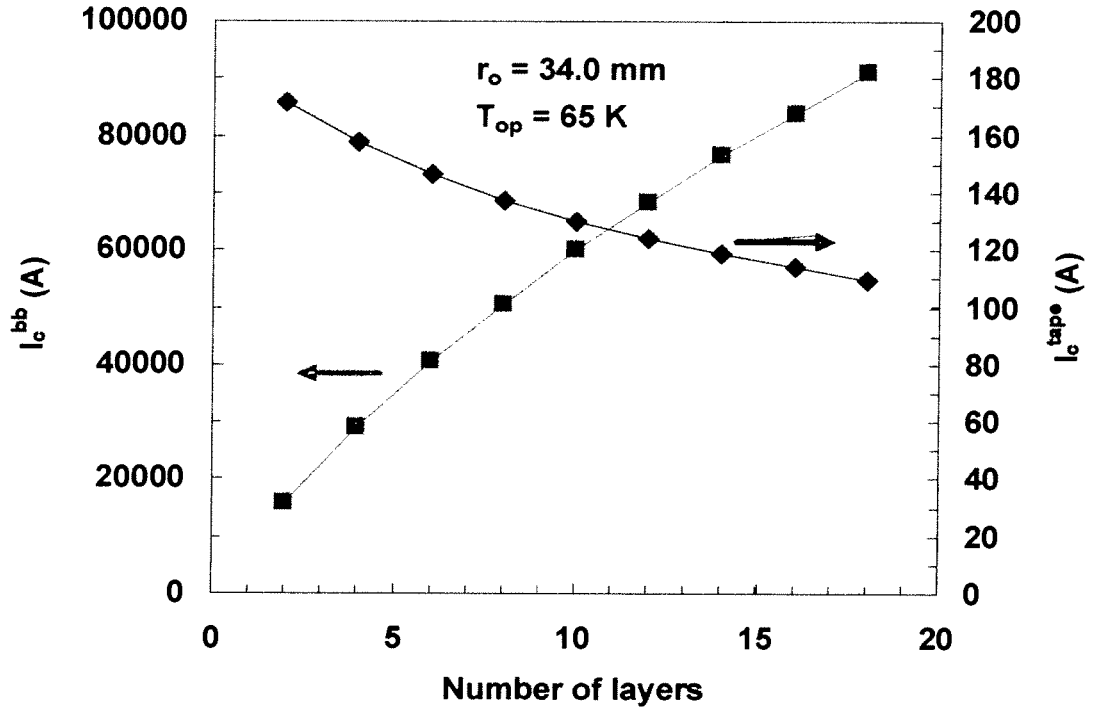

Figure 4-10. Bus bar and tape critical currents at 65 K as a function of the number of Bi-2223 layers wound onto a flexible stainless steel pipe of 34.0 mm outer radius.

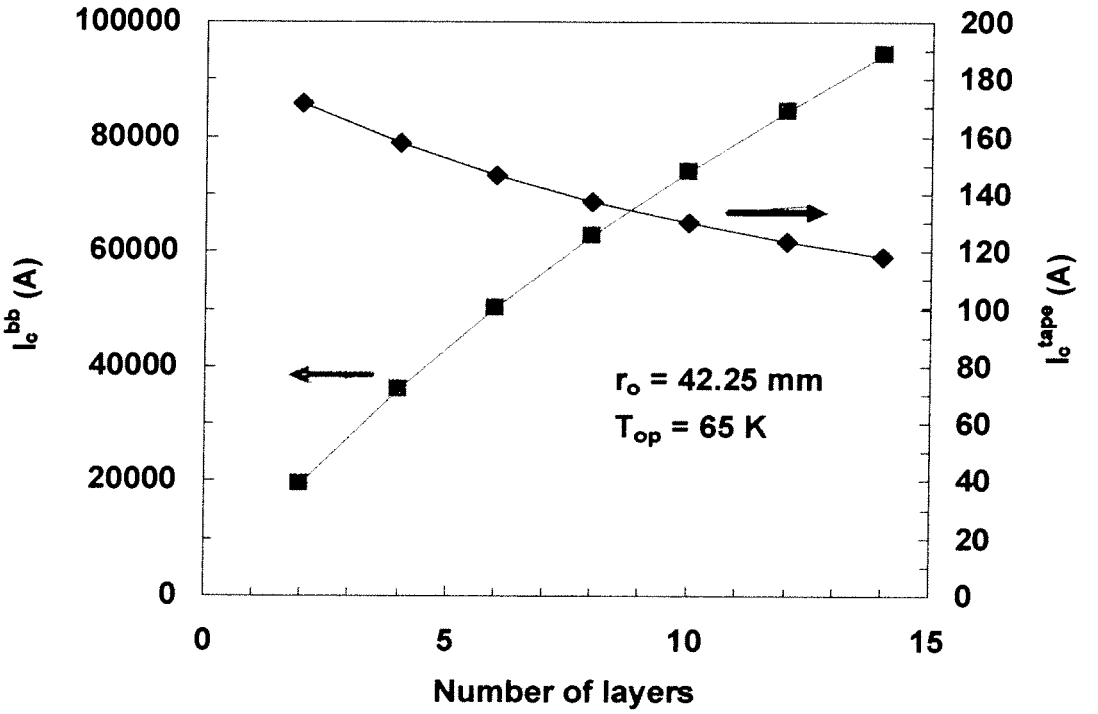

Figure 4-11. Bus bar and tape critical currents at 65 K as a function of the number of Bi-2223 layers wound onto a flexible stainless steel pipe of 42.25 mm outer radius.

4.3.2 Examples of TF and PF Bus Bar Designs

The bus bar designs presented in this section are based on the use of commercially available flexible stainless steel pipes. The maximum conductor temperature is limited to 65 K. The main dimensions and the operating conditions for the investigated design options are presented in Table 4-5.

Table 4-5. HTS bus bar designs based on the dimensions of commercially available flexible stainless steel pipes.

HTS Bus Bar Designs						
Design	TF A	TF B	TF C	PF A	PF B	PF C
Former						
r_i / r_o [mm]	25.0 / 26.5	32.5 / 34.0	40.0 / 42.25	25.0 / 26.5	32.5 / 34.0	40.0 / 42.25
Superconductor	AgMg/Ag/Bi-2223 tapes (4 mm ? 0.22 mm), I_c(77 K, sf) =115 A					
Tapes/layer n	35	46	57	35	46	57
Number of layers N	24	16	12	16	12	8
r_{sc} [mm]	31.78	37.52	44.89	30.02	36.64	44.01
Thermal insulation						
r_{1ith} / r_{2ith} [mm]	38.1 / 42.8	49.0 / 54.6	49.0 / 54.6	38.1 / 42.8	49.0 / 54.6	49.0 / 54.6
r_{1oth} / r_{2oth} [mm]	63.5 / 71.45	73.5 / 81.25	73.5 / 81.25	63.5 / 71.45	73.5 / 81.25	73.5 / 81.25
Electrical insulation						
r_{id} / r_{od} [mm]	71.45/80.76	81.25/90.49	81.25/90.49	71.45/80.76	81.25/90.49	81.25/90.49
Operating conditions						
T_{op} [K]	**65**	**65**	**65**	**65**	**65**	**65**
I_{op} [kA]	68	68	68	45(52)	45(52)	45(52)
I_c [kA]	**86**	**84**	**84.5**	**65**	**68.5**	**62.5**
U [kV]	17.5	17.5	17.5	17.5	17.5	17.5
E_m [kV/mm]	2	2	2	2	2	2
Losses						
P_{AC} [W/m]	-	-	-	0.012	0.008	0.004
P_{th} [W/m]	0.75	0.99	0.99	0.75	0.99	0.99

In the case of the TF coils a critical current of approximately 85 kA seems to be sufficient for a safe operation of the bus bars. The number of Bi-2223 layers needed to reach a critical current of 85 kA depends on the outer radius of the flexible stainless steel pipe used as cable former. For an outer radius of 42.25 mm 12 layers of Bi-2223 tapes are sufficient to reach a critical current of 84.5 kA at an operating temperature of 65 K (Design TF C). The outer radius of the bus bar varies between 80.76 (TF A) and 90.49 mm (TF B & C). The heat leak through the thermal insulation varies between 0.75 and 0.99 W/m. The length of the TF bus bars is approximately 12 m [23]. The resulting total thermal load for a single TF bus bar is ≈12 W.

The bus bars will be cooled using helium gas of 50 K inlet temperature. Figure 4-12 shows the specific heat of helium gas as a function of pressure and temperature. For pressures in the range of 1 to 10 bars and temperatures between 50 and 90 K the specific heat depends only weakly on temperature and pressure. To estimate the required helium mass flow rate, a specific heat of 5.2 J/g K is used. Allowing an increase of the helium temperature from 50 to

51 K the helium mass flow rate required to remove the thermal heat load of approximately 12 W is

$$\dot{m} = \frac{P}{C_p \Delta T} = \frac{12\text{W}}{5.2\text{J/gK} \cdot 1\text{K}} = 2.31\text{g/s} \tag{12}$$

The helium gas used to cool the TF bus bar may also be used to cool the conventional current lead operating between ≈65 K and room temperature. During the extended tests of the 70 kA HTS current lead [6], it was found that a 50 K helium mass flow rate of 4.7 g/s is necessary to cool the heat exchanger part of the current lead at the nominal current of 68 kA. This result indicates that the use of TF HTS bus bars does not significantly enhance the required 50 K helium mass flow rate. Using both, HTS bus bars and current leads, the warm end temperature of the HTS bus bar should be kept at a temperature of 65 K even during stand-by operation. Therefore, the required helium mass flow rate at stand-by operation cannot be reduced to 1.0 g/s as in the case of the 70 kA HTS current lead, where a warm end temperature of 105 K may be acceptable.

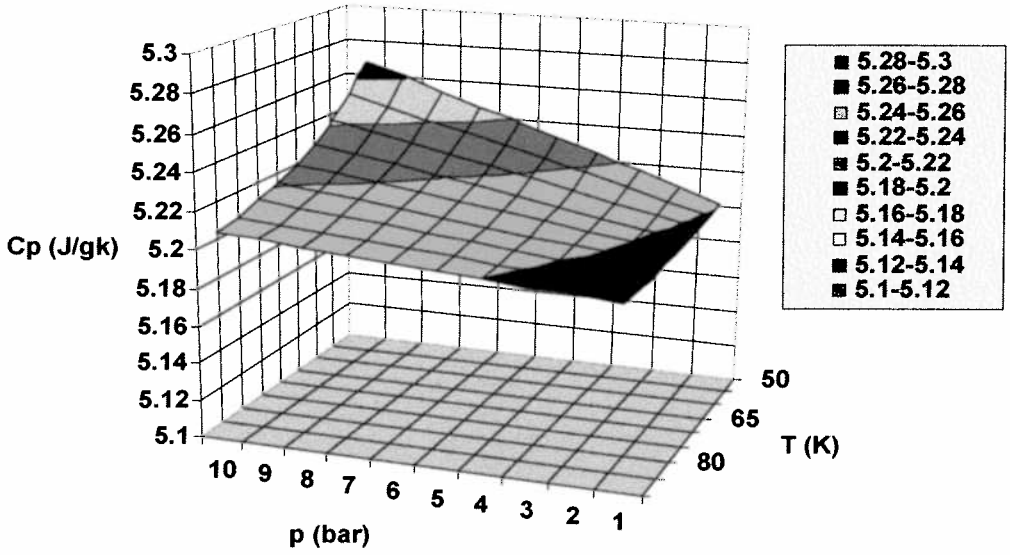

Figure 4-12. Specific heat of helium gas as a function of pressure and temperature. In the considered pressure and temperature range the specific heat is close to 5.2 J/g K.

For the PF coils a bus bar critical current well above 60 kA seems to be sufficient even for the operation in back-up mode. For the former of 42.25 mm outer radius 8 layers of Bi-2223 tapes are necessary to reach a critical current of 62.5 kA at an operating temperature of 65 K. The outer radius of the bus bar varies between 80.76 (PF A) and 90.49 mm (PF B & C). Due to the pulsed operation of the PF and CS coils the transport current AC losses need to be taken into consideration. The AC losses averaged over a plasma cycle of 1800 s length were estimated using the monoblock model. In the case of a uniform current distribution the AC losses may be considerably lower. In the calculation of the AC losses a variation of the current from 45 kA to -45 kA and back to 45 kA was assumed. For all considered PF/CS bus bar designs the AC loss averaged over a full cycle of 1800 s is lower than 0.012 W/m, which is by more than a factor of 60 smaller than the thermal losses. Taking into account that the highest values

of the field change rate reach more than 60 times the average value of 50 A/s (2×45000 A/1800 s = 50 A/s) (see reference scenarios according to Tables 4-1 and 4-2) the peak load due to the AC losses may become comparable to the thermal losses for a duration of less than 10 seconds. Nevertheless, the mass flow rate required to cool the bus bars under pulsed operation is expected to be not significantly higher than that necessary to cool only a current lead.

During the test of the 70 kA HTS current lead the voltage measurements were affected by the 600 Hz ripple of the power supply. The question arises, if the 600 Hz ripple of the power supply causes AC losses in the HTS bus bars. In the case of the PF and CS coils the AC losses due to the pulsed operation are expected to be much larger than the 600 Hz ripple losses. Long flat-top times are only foreseen for the TF coil system of ITER. It is therefore sufficient to consider the TF coils. To reduce the voltage ripple the power supply is alternatively connected to the 69 and the 22 kV power grids. The maximum voltage of the power supply is 900 V, where the phase angle is close to 90°. Using a value of 0.1 for $\cos\delta$ leads to an inductive voltage V_L = 900 V × 0.1 × 22/69 = 28.7 V. The inductance of the 18 TF coils is 17.7 H leading to an inductive resistance $R_L = \omega L = 2\pi f L$ = 66.7 kΩ (f = 600 Hz). Thus, the ripple current is $\Delta I = V_L/R_L$ = 28.7 V / 66.7 kΩ = 0.43 mA. Consequently the ripple current is only of the order 10^{-8} of the transport current of 68 kA. Based on this estimation it can be expected that the AC losses caused by the 600 Hz ripple of the power supply would be negligible in the ITER HTS bus bars.

4.3.3 Optimized HTS TF and PF Bus Bar Designs

The use of corrugated stainless steel pipes with dimensions optimized for the bus bar application would reduce the outer dimensions of the HTS bus bars for ITER. In addition, it seems to be possible to enhance the maximum electric field in the dielectric up to a value of 5 kV/mm. The outer radii of the corrugated stainless steel pipes envisaged to be used for the thermal insulation system obey the relation [24]

$$r_{op} = 1.104 r_{ip} + 0.39\,\text{mm} \tag{13}$$

where r_{ip} and r_{op} are the inner and outer radii in millimeter. It seems to be sufficient to have an inner radius of the inner wall of the thermal insulation, which is 3 mm larger than the outer radius of the outermost superconducting layer. The space needed for the evacuated superinsulation is 20 mm. The bus bar dimensions resulting for the use of flexible stainless steel pipes with optimum dimensions are listed in Table 4-6.

Using flexible stainless steel pipes with optimized dimensions the outer radii of TF and PF HTS bus bars can be reduced to 85 (TF C, 12 layers) and 75 mm (PF B, 12 layers), respectively. The cross-section of the HTS bus bars is by a factor of ≈2 smaller than that of the water-cooled Al bus bars. In the case that Bi-2223 tapes with I_c(77 K, sf) > 150 A would be available the number of layers in the designs TF B and PF A could be reduced to a reasonable value of 12. The outer bus bar radii accessible with these two designs would be 76 and 67 mm, respectively. The resulting reduction in the bus bar cross-sections would be between a factor of 2 and 3.

Table 4-6. HTS bus bar designs based on the dimensions of flexible stainless steel pipes with optimized dimensions.

HTS Bus Bar Designs

Design	TF A	TF B	TF C	PF A	PF B	PF C
Former						
r_i / r_o [mm]	25.0 / 26.5	32.5 / 34.0	40.0 / 42.25	25.0 / 26.5	32.5 / 34.0	40.0 / 42.25
Superconductor	AgMg/Ag/Bi-2223 tapes (4 mm ? 0.22 mm), I_c(77 K, sf) =115 A					
Tapes/layer n	35	46	57	35	46	57
Number of layers N	24	16	12	16	12	8
r_{sc} [mm]	31.78	37.52	44.89	30.02	36.64	44.01
Thermal insulation						
r_{1ith} / r_{2ith} [mm]	34.78/38.79	40.52/45.12	47.89/53.26	33.02/36.84	39.64/44.15	47.01/52.29
r_{1oth} / r_{2oth} [mm]	58.79/65.29	65.12/72.28	73.26/81.27	56.84/63.14	64.15/71.21	72.29/80.20
Electrical insulation						
r_{id} / r_{od} [mm]	65.29/68.89	72.28/75.87	81.27/84.85	63.14/66.74	71.21/74.80	80.20/83.78
Operating conditions						
T_{op} [K]	**65**	**65**	**65**	**65**	**65**	**65**
I_{op} [kA]	68	68	68	45(52)	45(52)	45(52)
I_c [kA]	**86**	**84**	**84.5**	**65**	**68.5**	**62.5**
U [kV]	17.5	17.5	17.5	17.5	17.5	17.5
E_m [kV/mm]	5	5	5	5	5	5
Losses						
P_{AC} [W/m]	-	-	-	0.012	0.008	0.004
P_{th} [W/m]	0.71	0.80	0.93	0.68	0.79	0.91

4.3.4 Minimum Bending Radii

For the water-cooled aluminium bus bars the minimum bending radii are in the ranges 428 to 1200 mm (TF) and 212 to 1200 mm (PF, CS) depending on whether the thicker or the thinner side of the rectangular bus bar is bent. The proposed HTS bus bar design is in principle flexible, however, the minimum tolerable bending radii are relatively large. The minimum tolerable bending radii for the proposed cable formers (not completely tight) and the Flexwell^{TM} tubes (vacuum tight corrugated stainless steel pipes) are listed in Table 4-7. It may be noticed that the minimum tolerable bending radius is not limited by the HTS tapes.

Table 4-7. Minimum tolerable bending radii for the cable formers (For) and the corrugated stainless steel pipes (Flex) needed for the thermal insulation system.

	For 1	For 2	For 3	Flex 1	Flex 2	Flex 3	Flex 4
Inner radius (mm)	25.0	32.5	40.00	38.1	49.0	63.5	73.5
Outer radius (mm)	26.5	34.0	42.25	42.8	54.6	71.45	81.25
Minimum bending radius (mm)	320	400	320	1400	1800	2300	2600

The flexibility of the HTS bus bars is limited by the minimum tolerable bending radii of the corrugated stainless steel pipes enclosing the evacuated superinsulation. The lowest tolerable bending radii of the corrugated stainless steel pipes Flex 1 and 4 are 1400 and 2600 mm, respectively.

4.3.5 Magnetic Field in the Bend Region

In the region of a bend the magnetic field is enhanced as compared to a straight conductor. In addition, field components perpendicular to the broad face of the Bi-2223 tapes are generated. The magnetic field for a bend of 1000 mm radius has been estimated for the bus bar design TF C. A sketch of the conductor arrangement is shown in Figure 4-13. In the calculation of the magnetic field the bus bar is represented by a single current line in the centre. The procedure is similar to that described in a previous report [25]. The results of the field calculations are presented in Table 4-8.

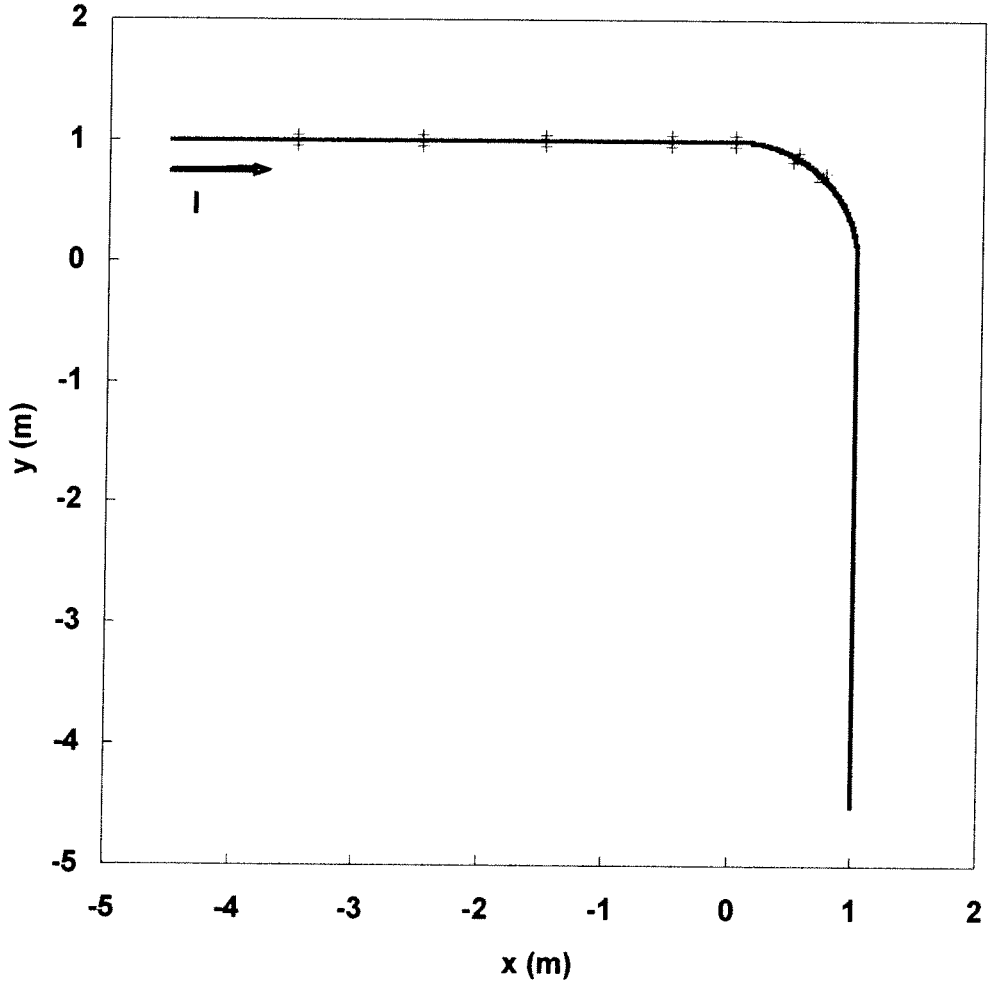

Figure 4-13. Conductor arrangement used for the estimation of the magnetic field at the positions marked by the crosses.

The magnetic field at the surface of the outermost superconducting layer of a straight TF bus bar, based on the design TF C, is 303 mT at the nominal current of 68 kA. The magnetic fields listed in Table 4-8 indicate that for a bend of 1000 mm radius the maximum field perpendicular to the broad face of the tapes is approximately 21 mT at a current of 68 kA. The maximum magnetic field is reached in the centre of the bend region. The maximum tangential field reaches a value of ≈331 mT at a current of 68 kA. The critical current in the bend region at a temperature of 65 K is limited by the enhanced tangential field and not by the additional field component perpendicular to the broad face of the tapes. The reduction of the tape critical current due to the enhanced tangential field is less than 5 %. Consequently the minimum tolerable bending radius of the HTS bus bars is not limited by the field enhancement in the region of the bend for a bending radius of 1000 mm.

Table 4-8. Estimated magnetic field (B_x, B_y, B_z) at the positions (x, y, z) for I = 68 kA. $B_\perp$ is the field component perpendicular to the broad face of the tapes.

x (m)	*y (m)*	*z (m)*	*B_x (mT)*	*B_y (mT)*	*B_z (mT)*	*$B_\perp$ (mT)*
-3.5	1.04489	0	0	0	301.63	0
-3.5	0.95511	0	0	0	-304.00	0
-3.5	1	0.04489	-0.01	-302.80	-1.19	-1.19
-3.5	1	-0.04489	0.01	302.80	-1.19	1.19
-2.5	1.04489	0	0	0	301.25	0
-2.5	0.95511	0	0	0	-304.61	0
-2.5	1	0.04489	-0.02	-302.91	-1.68	-1.68
-2.5	1	-0.04489	0.02	302.91	-1.68	1.68
-1.5	1.04489	0	0	0	300.36	*0*
-1.5	0.95511	0	0	0	-305.60	*0*
-1.5	1	0.04489	-0.05	-302.92	-2.60	-2.60
-1.5	1	-0.04489	0.05	302.92	-2.60	2.60
-0.5	1.04489	0	0	0	*294.17*	*0*
-0.5	0.95511	0	0	0	*-304.55*	*0*
-0.5	1	0.04489	-0.23	-302.87	-5.18	-5.18
-0.5	1	-0.04489	0.23	302.87	-5.18	5.18
0	1.04489	0	0	0	281.27	0
0	0.95511	0	0	0	-314.55	0
0	1	0.04489	-6.80	-297.01	-13.22	-13.22
0	1	-0.04489	6.80	297.01	-13.22	13.22
0.52245	0.90490	0	0	0	276.30	0
0.47756	0.82715	0	0	0	-331.04	0
0.5	0.86603	0.04489	-151.46	-261.55	-20.51	-20.51
0.5	0.86603	-0.04489	151.46	261.55	-20.51	20.51
0.72955	0.72955	0.03174	-148.92	-148.66	190.35	-14.20
0.68466	0.68466	-0.03174	153.68	153.41	-238.98	15.44
0.72955	0.72955	-0.03174	148.92	148.66	190.35	14.20
0.68466	0.68466	0.03174	-153.68	-153.41	-238.98	-15.44
0.70711	0.70711	0.04489	-213.89	-213.52	-20.87	-20.87
0.70711	0.70711	-0.04489	213.89	213.52	-20.87	20.87
0.73885	0.73885	0	0	0	272.94	0
0.67536	0.67536	0	0	0	-331.35	0

4.3.6 Magnetic Field of the Return Conductor

For a single conductor the self-field is always tangential to the conductor surface, i.e. the magnetic field is parallel to the broad face of the Bi-2223 tapes. In the case of the TF bus bar design TF C the outer radius of the superconducting layers is 44.89 mm. The self-field generated by a single conductor at the nominal current is 0.303 T. The outer diameter of the bus bar is approximately 170 mm. Taking into consideration the return conductor, its stray field has field components parallel and perpendicular to the broad face of the tapes. Assuming, that the distance of the return conductor is 300 mm, the contribution of the return conductor to the maximum magnetic field parallel to the broad face of the Bi-2223 tapes is 0.053 T. The resulting maximum tangential magnetic field is 0.356 T. The maximum magnetic field perpendicular to the broad face of the tapes is 0.0464 T. The tape critical currents at 65 K in tangential magnetic fields of 0.303 and 0.356 T are 134.5 and 126.6 A, respectively. On the other hand, the tape critical current at 65 K for a magnetic field of 0.0464 T, perpendicular to the broad face of the tapes, is 145 A. Thus, the critical current is not limited by the small field perpendicular to the broad face of the tapes generated by the return conductor. The bus bar critical current at an operating temperature of 65 K is reduced from 84.5 to 80.3 kA. Thus, the enhancement of the tangential magnetic fields leads only to a 5 % reduction of the bus bar critical current.

4.3.7 Fault Currents

The short circuit currents in the TF and PF bus bars reach values of 300 and 200 kA, respectively. Because of cost reasons, the HTS bus bar can not be designed to be able to carry such high currents. The problem of the handling of the short circuit currents needs to be investigated in more detail. Using a superconducting fault current limiter, as has been proposed for HTS power transmission cables, may be used to solve the problem. However, the use of a HTS fault current limiter would further enhance the investment costs.

4.4 Economic Aspects

The required length of Ag/Bi-2223 tapes and the corresponding conductor costs for a 12 m long TF bus bar are listed in Table 4-9. The estimation of the superconductor costs is based on a price of 60 € per meter of Ag/Bi-2223 tape. The required length of the tapes is by a factor $1/\cos\varphi$ larger than the length of the bus bar because of the twist pitch. In the present cost estimation, a twist angle of 30° is used. In principle, the required length of the tapes is further enlarged because of the material needed for the forerun in the winding process. This additionally required material has been neglected in the estimation presented in Table 4-9.

Table 4-9. Conductor costs for a HTS bus bar of 12 m length.

Design	TF A	TF B	TF C
Number of tapes	840	736	684
Length of tape [m]	11640	10200	9480
Tape costs [k€]	698	612	569
Critical current [kA]	86	84	84.5
Costs/current/length [k€/kA/m]	0.676	0.607	0.561

The superconductor costs have to be compared to the costs of an aluminium bus bar of 12 m length. It seems to be reasonable to assume that the costs for the ITER TF bus bars would be comparable to those for the 80 kA bus bars installed for the 70 kA HTS current lead test at the Forschungszentrum Karlsruhe. The numbers are as follows [26]:

Engineering design, drawings etc.	42.0 k€
Material, fabrication including water cooling, assembly leak and insulation tests	6.40 k€/m

The estimated total cost for an ITER TF aluminium bus bar of 12 m length would be approximately 100 k€, which is by a factor of 5 to 6 less than the costs for the Bi-2223 tapes.

The operating costs for a HTS TF bus bar combined with an HTS current lead are not significantly higher than those for the HTS current lead alone. The Joule heat generated in the aluminium bus bars at the nominal current of 68 kA is 3.4 kW/m (see Section 4.2). For a bus bar of 12 m length, the electric losses are as high as 40.8 kW. Based on a duty cycle of 32 % the operating time within one year is 8760 h × 0.32 = 2803 h. The electric energy consumed by a single TF bus bar of 12 m length within one year is therefore 40.8 kW × 2803 h = 114362 kWh. The electricity costs per single TF bus bar and year reach a value of ≈5700 € for an energy price of 0.05 €/kW h. If we assume that the costs for the water cooling are comparable to the electricity costs, the operating costs for a single bus bar are of the order of 12 k€ per year. The accumulated operating costs over an operation time of 20 years would reach 240 k€ for a single TF bus bar. The potential savings in operation costs seem to be smaller than the additional investment costs caused by the use of HTS bus bars.

4.5 High Operating Temperature Option

The thermal shields of ITER will be cooled by helium gas of 80 K inlet temperature. It would therefore be desirable to use this helium gas also to cool the HTS current leads and bus bars. Very recently, it has been demonstrated that the 70 kA EU HTS current lead demonstrator for the TF coils of ITER could be operated in steady state even for a helium inlet temperature of 80 K. This result clearly indicates that the HTS current leads for ITER could be operated using the 80 K helium gas available in a large quantity for the shield cooling. In order to provide the required safety margins the average magnetic field perpendicular to the broad face of the tapes has to be reduced. Moreover, the superconductor cross-section needs to be increased. In principle a further improvement of the critical current of the AgAu/Bi-2223 tapes seems to be possible.

For this reason the operation of the HTS bus bars with warm end temperatures between 80 and 85 K has been considered. The results of these estimations have been described in a previous report [27]. The main result of this estimation is that for a former diameter of 68 mm diameter, 38 layers of Ag/Bi-2223 tapes would be required for an operating temperature of 80 K. It seems to be not feasible to wind such a large number of layers onto a cable former. In addition, severe problems in the current distribution among the layers may occur. The required amount of superconductor is mainly determined by the operation temperature. Operating temperatures of 80 K or above would lead to unreasonably high superconductor costs of more than 1.5 M€ for a single TF bus bar of 12 m length.

4.6 Conduction-Cooled HTS Bus Bars

For the DC bus bars of the TF coil system the possibility to use conduction-cooled HTS bus bars has been considered. To reduce the thermal conductivity of the matrix gold is added to the silver matrix of Bi-2223 tapes used for the current lead application. The thermal conductivity of pure silver integrated over the temperature range of 4 to 80 K is by a factor of 20 larger than that of AgAu. Using Bi-2223 tapes with a pure silver matrix it would in principle to be possible reach a length of 12 m for the HTS part of the current lead [28]. Nevertheless, it seems to be difficult to replace the HTS part of the current lead (AgAu/Bi-2223) and the water-cooled aluminium bus bars by a conduction-cooled Ag/Bi-2223 current lead of approximately 12 m length. The main problem encountered is the presence of bends in the TF bus bars for ITER, which would require a flexible design. In addition, the fabrication of Bi-2223 stacks by a sintering process is limited by the length of the furnaces used in the fabrication process. Using a soldering process it may possible to prepare sufficiently long stacks, however, this process has not yet been demonstrated.

5. Conclusions

In the present report the conceptual design of HTS bus bars, which is similar to that used for HTS power transmission cables, has been presented. To reach a reasonably small number of layers it is necessary to operate the bus bars at temperatures of 65 K or below. Using flexible stainless steel pipes of optimized dimensions, the cross-section of the HTS bus bars may be reduced by a factor of 2-3 as compared to the water-cooled Al bus bars. Even for an operating temperature of 65 K, the HTS costs exceed 500 k€. This conductor cost is based on the assumption of a price of 60 € per meter of Ag/Bi-2223 tape. In the conductor layout and the cost estimation, a self-field critical current of 115 A at 77 K has been supposed. The uncertainty of the in-field critical current at 65 K and the bus bar self-field is approximately 20 %. The availability of Ag/Bi-2223 tapes with I_c values above 150 A at 77 K and zero applied field would provide the possibility to reduce the number of layers or the former diameter. A reduced former diameter would allow the reduction of the HTS bus bar dimensions. In addition, higher performance tapes could lead to reduced superconductor costs.

In last few years, a remarkable improvement of the properties of long, developmental YBCO-123 coated conductors has been achieved. The use of Y-123 coated conductors with superior properties may provide a reduced number of layers as well as reduced superconductor costs. Because of the fact that Y-123 coated conductors are presently not commercially available in long length, a HTS bus bar design based on the use of coated conductors has not been investigated within the framework of this task.

The heat leak of the order of 1 W/m has been found to be the main loss contribution. The AC loss in the PF and CS bus bars averaged over a full plasma cycle has been found to be negligible as compared to the thermal losses. The cooling power required for a combination of HTS bus bar and current lead is expected to be not significantly larger than that necessary to cool only the HTS current lead. Based on the present Bi-2223 performance (I_c(77 K, sf) = 115 A) and conductor prices (60 €/m) the savings in the operation costs within 20 years of operation are expected to be smaller than the additional investment costs caused by the use of HTS bus bars.

The minimum tolerable bending radius is for most of the proposed designs, which are based on the use of commercially available flexible stainless steel pipes, between 2.3 and 2.6 m. The minimum bending radius is determined by the flexible stainless steel pipes providing the vacuum for the thermal insulation system. In principle it would be possible to bend the cable former on bending radii of less than 1 m. The field enhancement in the bend region was found to be not a limiting factor. A distance of the return conductor of 300 mm seems to be reasonable.

Using flexible stainless steel pipes optimized for the bus bar application and higher performance tapes the total diameter of the HTS TF bus bars may be reduced to ≈152 mm, corresponding to a cross-section of ≈18000 mm^2. The dimensions of a water-cooled TF aluminium bus bar are 236 mm × 217 mm, corresponding to a total cross-section of 51200 mm^2.

The main advantage of the use of HTS bus bars instead of water-cooled aluminium bus bars could be the reduction of the required cross-sections. For the use of HTS bus bars it would be desirable to have a limited number of bends with a sufficiently large bending radius.

The design of the terminations and the aspects related to the large short circuit currents have to be investigated in further studies.

6. Acknowledgement

This work has been performed in the frame of the European Fusion Technology Programme under Task EFDA TW4-TMSF-HTSCOM.

7. References

1. R. Heller, S.M. Darweschsad, G. Dittrich, W.H. Fietz, S. Fink, W. Herz, A. Lingor, A. Kienzler, I. Meyer, G. Nöther, M. Süsser, V.L. Tanna, R. Wesche, F. Wüchner, and G. Zahn, *Interner Bericht FE.5130.0061.0012/A, Test of the 70 kA HTS Current Lead in the TOSKA Facility – Results of test phases I and II,* Forschungszentrum Karlsruhe, September 2004.

2. R. Heller, G. Friesinger, A.M. Fuchs, and R. Wesche, *Development of High Temperature Superconductor Current Leads for 70 kA,* **IEEE Transactions Appl. Supercond. 12** (2002) 1285-1288.

3. R. Heller, D. Aized, A. Akhmetov, W.H. Fietz, F. Hurd, J. Kellers, A. Kienzler, A. Lingor, J. Maguire, A. Vostner, and R. Wesche, *Design and Fabrication of a 70 kA Current Lead Using Ag/Au Stabilized Bi-2223 Tapes as a Demonstrator for the ITER TF-Coil System,* **IEEE Transactions Appl. Supercond. 14** (2004) 1774-1777.

4. R. Heller, S.M. Darweschsad, G. Dittrich, W.H. Fietz, S. Fink, W. Herz, F. Hurd, A. Kienzler, A. Lingor, I. Meyer, G. Nöther, M. Süsser, V.L. Tanna, A. Vostner, R. Wesche, F. Wüchner, and G. Zahn, *Experimental Results of a 70 kA High Temperature Superconductor Current Lead Demonstrator for the ITER Magnet System,* Paper 4LL05 presented at the Applied Superconductivity Conference 2004 in Jacksonville.

5. R. Wesche, *LRP 720/02 Thermodynamic Optimisation of 70 kA Binary Current Lead (Final Report),* Centre de Recherches en Physique des Plasmas, February 2002.

6. R. Heller, R. Wesche, M. Borlein, S.M. Darweschsad, G. Dittrich, W.H. Fietz, S. Fink, W. Herz, A. Kienzler, A. Lingor, I. Meyer, M. Süsser, V.L. Tanna, F. Wüchner, and G. Zahn, *Interner Bericht FE.5130.0060.0012/A, Report on the Phase III Operation of the 70 kA HTS Current Lead,* Forschungszentrum Karlsruhe, June 2005.

7. ITER Design Document, *Plant Description: Tokamak System Design and Assessment, G A0 FDR 1 01-07-13 R1.0.*

8. ITER Design Document, *Site Layout and Buildings, G A0 FDR 1 01-07-13 R1.0.*

9. ITER DDD 4.1, *Pulsed Power Supplies, Appendix-A, N 41 DDD 18 01-07-06 R 0.3,* pp. 35-37.

10. ITER Design Description Document DDD 11, *Magnet Report no. (N11 DDD 177 04-05-12 W 0.2).*

11. ITER superconducting Magnet and Electrical design guideline level 1, *N11 FDR 1201-07-02 R 0.1,* July 2001, 1-75.

12. R. Heller, W.H. Fietz, R. Lietzow, V.L. Tanna, R. Wesche, and G. Zahn, *Interner Bericht FE.5130.0060.0012/B, Report on the Comparison of ITER Design with and without HTS Current Leads, EFDA No. TW4-TMSF-HTSCOM, Deliverable 1,* Forschungszentrum Karlsruhe, June 2005.

13. R. Heller, S.M. Darweschsad, G. Dittrich, W.H. Fietz, S. Fink, W. Herz, A. Lingor, A. Kienzler, I. Meyer, G. Nöther, M. Süsser, V.L. Tanna, R. Wesche, F. Wüchner and G. Zahn, *Final Report on the Test of the 70 kA HTS Current Lead in the TOSKA Facility Contract No. FU05 CT 2003-00023 (EFDA No. 02-1013) Deliverable 4.2, Internal Report FE.5130.0061.0012/A*, Forschungszentrum Karlsruhe, October 2004, unpublished.

14. ITER document *N 41 DDD 16 01-07-06 R 0.3*, drawings *41 0040 0001, 41 0044 0001.*

15. ITER document *N 11 DDD 177 04-05-12 W 0.2, DDD 11 Magnet*, p.51.

16. J. Rieger et al., **Supercond. Sci. Technol. 11** (1998) 902-908.

17. M. Leghissa et al., **IEEE Trans. Appl. Supercond. 9** (1999) 406-411.

18. S. Krüger et al., **IEEE Trans. Appl. Supercond. 9** (1999) 833-836.

19. ITER document *N 11 DDD 177 04-05-12 W 0.2, DDD 11 Magnet*, pp. 42-45.

20. W.T. Norris, **J. Phys. D 3** (1970) 489-507.

21. T. Fukunuga et al., **Appl. Phys. Lett. 66** (1995) 2128-2130.

22. R. Wesche, **Physica C 246** (1995) 186-194.

23. ITER document *N 41 SP 23 00-07-19 W 0.1, Coil power supply and distribution, Procurement package #41.P3, Annex 1*, p. 19.

24. R. Wesche, A. Anghel, B. Jakob, G. Pasztor, R. Schindler, G. Vécsey, **Cryogenics 39** (1999) 767-775.

25. R. Wesche, *Internal Report, Calculation of the Stray Magnetic Field at the Hall Probes of the HTS Current Lead Module*, Centre de Recherches en Physique des Plasmas, November 5, 2003.

26. M.S. Darweschsad, private communication

27. R. Wesche, *Internal Report, Conceptual Design of HTS Bus Bars for ITER*, Centre de Recherches en Physique des Plasmas, March 29, 2005.

28. R. Wesche, *Internal Report, Conduction-Cooled DC Bus Bar*, Centre de Recherches en Physique des Plasmas, February 21, 2005.